

DISCRETE BIFURCATION DIAGRAMS AND PERSISTENCE

A THESIS SUBMITTED TO
THE GRADUATE SCHOOL OF NATURAL AND APPLIED SCIENCES
OF
MIDDLE EAST TECHNICAL UNIVERSITY

BY

TÜRKMEN ÖRNEK

IN PARTIAL FULFILLMENT OF THE REQUIREMENTS
FOR
THE DEGREE OF DOCTOR OF PHILOSOPHY
IN
MATHEMATICS

AUGUST 2018

Approval of the thesis:

DISCRETE BIFURCATION DIAGRAMS AND PERSISTENCE

submitted by **TÜRKMEN ÖRNEK** in partial fulfillment of the requirements for the degree of **Doctor of Philosophy in Mathematics Department, Middle East Technical University** by,

Prof. Dr. Halil Kalıpçılar
Dean, Graduate School of **Natural and Applied Sciences**

Prof. Dr. Yıldray Ozan
Head of Department, **Mathematics**

Assoc. Prof. Dr. Semra Pamuk
Supervisor, **Mathematics Department, METU**

Examining Committee Members:

Prof. Dr. Yıldray Ozan
Mathematics Department, METU

Assoc. Prof. Dr. Semra Pamuk
Mathematics Department, METU

Assist. Prof. Dr. Pınar Mete
Mathematics Department, Balıkesir University

Assoc. Prof. Dr. M. Fırat Arıkan
Mathematics Department, METU

Assist. Prof. Dr. Elif Medetoğulları
Mathematics Department, Atılım University

Date:

I hereby declare that all information in this document has been obtained and presented in accordance with academic rules and ethical conduct. I also declare that, as required by these rules and conduct, I have fully cited and referenced all material and results that are not original to this work.

Name, Surname: TÜRKMEN ÖRNEK

Signature :

ABSTRACT

DISCRETE BIFURCATION DIAGRAMS AND PERSISTENCE

Örnek, Türkmen

Ph.D., Department of Mathematics

Supervisor : Assoc. Prof. Dr. Semra Pamuk

August 2018, 69 pages

Let $f_{t_i} : M \rightarrow \mathbb{R}$ be a discrete Morse function on a cell complex M for each $t_0 < t_1 < \dots < t_n = 1$. Let us denote slice as $M_i = M \times \{t_i\} \subset M \times I$ and let V_i be the discrete vector field on each slice. After extending the discrete vector field on each slice to a discrete vector field on all of $M \times I$, a discrete bifurcation diagram is obtained by connecting critical cells of the slices.

In "Birth and Death in Discrete Morse Theory" (King, Knudson, Mramor), a solution about finding the discrete bifurcation diagram has been presented. In this article, two cases have been researched. In the first case, triangulation of each slice is the same and $M \times I$ is regularly cell decomposed. For the first case, there is a known algorithm about extending discrete vector field on each slice to a gradient vector field on all of $M \times I$. In the second case, triangulation on each slice of cell complex M is different. It has seen that the way to extend the vector field on each slice to the vector field on all of $M \times I$ is not obvious. In this case, we have to choose a cell structure of $M \times I$ compatible with slices. The algorithm how one could define a discrete vector field on the resulting cell complex which does not have any closed paths is not known.

In this thesis, we intend to explain how to define the extended vector field when the triangulation on M is different and obtain the discrete bifurcation diagram. Furthermore, we want to get discrete bifurcation diagrams by using the persistence diagrams and compare these two discrete bifurcation diagrams.

Keywords: Discrete Morse Theory, Persistence Homology, Persistence Diagram, Discrete Bifurcation Diagram

ÖZ

AYRIK DALLANMA DİYAGRAMLARI VE İSTİKRARLILIK

Örnek, Türkmen
Doktora, Matematik Bölümü
Tez Yöneticisi : Doç. Dr. Semra Pamuk

Ağustos 2018 , 69 sayfa

M hücre kompleksi üzerinde her bir $t_0 < t_1 < \dots < t_n = 1$ için, $f_{t_i} : M \rightarrow \mathbb{R}$ ayrık Morse fonksiyon olsun. Her bir parçayı $M_i = M \times \{t_i\} \subset M \times I$ olarak gösterelim ve V_i her parça üzerindeki ayrık vektör alanları olsun. Her bir parça üzerindeki ayrık vektör alanlarını, $M \times I$ 'daki tüm ayrık vektör alanlarına genişlettikten sonra parçalar üzerindeki kritik hücreler birleştirilerek ayrık dallanma diyagramları elde edilir.

King, Knudson, Mramor'un "Birth and Death in Discrete Morse Theory" isimli makalesinde ayrık dallanma diyagramlarının bulunması ile ilgili bir çözüm verilmektedir. Bu makalede iki durum araştırılmıştır. Birinci durumda, her bir parça üzerindeki ayrıştırma aynıdır ve $M \times I$ düzgün bir şekilde hücrelere ayrıştırılmıştır. Birinci durum için, parça üzerindeki vektör alanlarını $M \times I$ üzerindeki düşüm vektör alanlarına genişletmesi ile ilgili bilinen bir algoritma vardır. İkinci durumda, her bir parça üzerinde hücre ayrıştırması farklıdır. Her parça üzerindeki vektör alanının $M \times I$ üzerindeki ayrık vektör alanına nasıl genişletildiğinin açık olmadığı görülmüştür. Bu durumda $M \times I$ için hücre yapısını parçalarla uyumlu olacak şekilde seçmemiz gerekiyor. Hücre kompleksi üzerinde kapalı yol oluşturmayacak şekilde ayrık vektör

alanının nasıl tanımlanacağını açıklayan bir algoritma bilinmemektedir.

Bizim bu tezdeki amacımız, M üzerindeki ayrıştırılmalar farklı iken, genişletilmiş vektör alanının nasıl tanımlanması gerektiğini anlatmak ve ayrık dallanma diyagramlarını elde etmektir. Ayrıca, istikrarlılık diyagramını kullanarak ayrık dallanma diyagramlarını bulmak ve bu iki ayrık dallanma diyagramlarını karşılaştırmaktır.

Anahtar Kelimeler: Ayrık Morse Teori, İstikrar Homoloji, İstikrar Diyagram, Ayrık Dallanma Diyagram

To memory of my mother and brother

ACKNOWLEDGMENTS

I would like to express my sincere gratitude to my advisor Associate Prof. Dr. Semra Pamuk for the continuous support of my Ph.D study and related research, for her patience, motivation, and immense knowledge. Her guidance helped me in all the time of research and writing of this thesis. I could not have imagined having a better advisor and mentor for my Ph.D study.

Besides my advisor, I would like to thank the rest of my thesis committee: Prof. Dr. Yıldırım Ozan, Assistant Prof. Dr. Pınar Mete for their insightful comments and encouragement, but also for the hard question which incited me to widen my research from various perspectives.

My sincere thanks also goes to Prof. Dr. Neza Mramor Kosta, who supports me to conduct this research.

Last but not the least, I would like to thank my family: to my father and brother and for supporting me spiritually throughout writing this thesis and my life in general.

TABLE OF CONTENTS

ABSTRACT	v
ÖZ	vii
ACKNOWLEDGMENTS	x
TABLE OF CONTENTS	xi
LIST OF FIGURES	xiii
LIST OF ABBREVIATIONS	xvii
CHAPTERS	
1 INTRODUCTION	1
2 BACKGROUND	3
2.1 Discrete Morse Theory	3
2.2 Bifurcation Diagram	9
2.2.1 Discrete Bifurcation Diagram	11
3 PERSISTENCE HOMOLOGY	19
3.1 Basic Definitions	19
3.2 Stability of Persistence Diagrams	25
3.3 Extended Persistence	35
4 THE PURPOSE OF THE STUDY AND METHOD	45
4.1 Method for the First Case	47

4.2	Method for the Second Case	58
4.3	Application	61
4.4	Conclusion	66
	REFERENCES	67
	CURRICULUM VITAE	69

LIST OF FIGURES

FIGURES

Figure 2.1 An example of a discrete Morse function	6
Figure 2.2 An example of a function which is not a discrete Morse function	6
Figure 2.3 The vector field of (a) is in figure (b)	8
Figure 2.4 Minimum, saddle and maximum critical simplices	8
Figure 2.5 The curves $f(x, t)$ for $t = -0.9, -0.04, 0.9, 1$	10
Figure 2.6 Bifurcation diagram of $f(x, t) = \frac{3x^4}{4} + \frac{x^3}{3} - \frac{tx^2}{2}$	11
Figure 2.7 Gradient vector field	13
Figure 2.8 A family of discrete gradient fields on the circle.	14
Figure 2.9 The connectivity diagrams associated with the example in Figure 2.8	15
Figure 2.10 (b) is the refinement of (a)	16
Figure 2.11 A family of discrete gradient fields on the circle with different triangulations.	17
Figure 2.12 The connectivity diagrams associated with the example 2.2.6	17
Figure 3.1 The sublevel set	19
Figure 3.2 The class ξ born at X_i since it does not lie in the (gray) image of H_q^{i-1} . The class ξ dies entering X_j since this is the first time its image merges into the image of H_q^{i-1}	21

Figure 3.3	Filtration	22
Figure 3.4	The sublevel set	22
Figure 3.5	Persistence diagrams of figure 3.4	23
Figure 3.6	The boundary matrix	24
Figure 3.7	Reduced boundary matrix	24
Figure 3.8	Close functions and persistence diagram	28
Figure 3.9	Homology group of the sublevel set $f^{-1}(-\infty, a]$	30
Figure 3.10	Image of F_a in F_b	30
Figure 3.11	Kernel of surjection of $F_a^b \rightarrow F_a^c$	31
Figure 3.12	Quotient of $F_a^{b,c}$ and $F_d^{b,c}$	31
Figure 3.13	Persistence diagram of f and g	33
Figure 3.14	Connectivity of persistence diagrams	34
Figure 3.15	The height function of torus	36
Figure 3.16	The reeb graph of torus	36
Figure 3.17	2-manifold torus	43
Figure 3.18	Ordinary persistence diagrams of dimension 0,1, and 2 from left to right	44
Figure 3.19	Extended persistence diagrams of dimension 0,1 and 2 from left to right	44
Figure 4.1	Discrete Morse functions F and G on circle from left to right	47
Figure 4.2	Persistence diagrams of 0-dimension	50
Figure 4.3	Persistence diagrams of 1-dimension	50

Figure 4.4	Overlaid persistence diagrams of 0-dimension	50
Figure 4.5	Ordinary, extended and relative persistence diagrams of F	51
Figure 4.6	Ordinary, extended and relative persistence diagrams of G	51
Figure 4.7	Overlaid persistence diagrams of F and G	52
Figure 4.8	A family of discrete gradient fields on circle	52
Figure 4.9	Connectivity diagrams associated with the example in figure 4.9	53
Figure 4.10	Strong connectivity diagrams associated with the example in figure 4.9	53
Figure 4.11	Discrete Morse function on circle	54
Figure 4.12	Discrete gradient fields	55
Figure 4.13	Discrete Morse function on torus	55
Figure 4.14	Persistence diagrams of $X \times \{t_i\}$	56
Figure 4.15	Persistence diagrams of $X \times \{t_{i+1}\}$	56
Figure 4.16	Connectivity diagrams associated with the example in figure 4.13	57
Figure 4.17	Extended persistence diagrams of dimension 1	57
Figure 4.18	A family of discrete gradient fields on circle with different cell decomposition	58
Figure 4.19	Discrete Morse functions on circle with different cell decomposition	59
Figure 4.20	Refinement process	59
Figure 4.21	Discrete Morse functions on circle with same cell decomposition	60
Figure 4.22	Blood of leukemic mouse	61
Figure 4.23	Image of leukemic cell	61
Figure 4.24	Image of leukemic cell	62

Figure 4.25 Connectivity diagrams associated with the application 62

LIST OF ABBREVIATIONS

$ K $	underlying space
K, M, X	simplicial complexes
$M, f : M \rightarrow \mathbb{R}$	manifold, Morse function
V	discrete vector field
$K_i = K \times \{t_i\}$	slice
v	vertex
$St(v)$	star of v
$Lk(v)$	link of v
$St_-(v)$	lower star of v
$Lk_-(v)$	lower link of v
$\alpha_1 * \alpha_2$	joining of simplices
N	refinement of a cell complex K
W	refinement of discrete vector field of V
X_i	the sublevel set
$\emptyset = X_0 \subset X_1 \subset \dots \subset X_n = X$	filtration
$i : A \hookrightarrow X$	inclusion map
$f_q^{i,j} : H_q(X_i) \rightarrow H_q(X_j)$	homomorphism map induced by inclusion map
$H_q^{i,j} = im(f_q^{i,j})$	q -th persistent homology
$\beta_q^{i,j}$	Betti number
$\mu_q^{r,s}$	multiplicity
$\overline{\mathbb{R}}^2$	Extended plane
$low(j)$	row index of the lowest 1 in column j
∂	boundary matrix
R	reduced boundary matrix

F_x	$H_i(f^{-1}(-\infty, x])$
f_x^y	the map from F_x to F_y
F_x^y	$Im f_x^y$
β_x^y	dimension of F_x^y
Δ	diagonal entries of persistence diagram
Q_a^b	closed upper left quadrant with corner (a, b)
$d_H(X, Y)$	Hausdorff distance
$d_B(X, Y)$	bottleneck distance
$Dgm(f)$	persistence diagram of f
X, Y	persistence diagrams
$R(f)$	Reeb Graph
$f_{\bar{u}}$	height function
M_a, M^a	sublevel set, superlevel set
$a_1 < a_2 < \dots < a_n$	homological critical values
$b_0 < b_1 < \dots < b_n$	interleaved values
$Ord_r(f)$	ordinary persistence diagram
$Rel_r(f)$	relative persistence diagram
$Ext_r(f)$	extended persistence diagram
K_j	subcomplex of K spanned by the first j vertices
L_{n-j}	subcomplex of K spanned by the last $n - j$ vertices
$h_p^{i,m}$	the map $H_p(K_i) \rightarrow H_p(K)$
K_p^i	$ker(h_p^{i,m})$

CHAPTER 1

INTRODUCTION

In 1920's Harold Calvin Marston Morse [18] introduced Morse theory which gives information about the topology of a smooth manifold. The main idea of the Morse theory is to build a bridge between the topology of the smooth manifold and the critical points of a smooth function on the manifold.

In 1990's Robin Forman [10] developed a discrete Morse theory as a combinatorial version of Morse theory. As in the Morse theory, the critical cells of a discrete Morse function determines the topology of the cell complex. [10, Theorem 2.5.] says that a simplicial complex K with a discrete Morse function is homotopy equivalent to a CW complex with exactly one cell of dimension p for each critical simplex of dimension p . There are several benefits of using discrete Morse theory in applications such as tracking features in a sequence of images [13], [20] and topological data analysis [3], [1]. Especially in image analysis and topological data analysis, there are algorithms to get rid of the noise [16], [8]; which is excess details of the image and data. These algorithms give us to work with simpler discrete Morse functions. For instance, in smooth Morse theory, a simpler Morse function can be obtained by cancelling gradient path between two critical points with two consecutive indices. We have an analogue of the same implementation in discrete setting; the cancellation of critical cell is done by reversing arrow between critical cells of successive dimensions.

The motivation of this thesis is finding a combinatorial version of the bifurcation diagrams in smooth setting by using persistence homology. An algorithm to draw the discrete bifurcation diagrams by using the discrete gradient vector fields is given in [14], which is called as the birth and death algorithm. Given a family of discrete Morse functions f_{t_j} on a simplicial complex K , let V_j denote the gradient vector

field of f_{t_j} . This algorithm finds which critical cells for the gradient vector field V_j correspond to which critical cells for V_{j+1} . When a new critical point emerges at some time t_j , the critical point is called “born”, if it disappears at other times, critical point is called “die”. Connectivity between critical cells in a discrete bifurcation diagram gives a way to follow the births and deaths of critical cells.

There are several subjects in discrete Morse theory and persistence homology that are closely related to each other. So, we draw the discrete bifurcation diagrams by using the persistence homology; which is a method that measures the topological features of shapes and functions. First, we need a filtration of the space to determine the birth and death of homology classes and then find persistence pairs. After sketching the persistence diagrams for each slice and each dimension, we use stability to sketch discrete bifurcation diagrams.

The overview of this thesis is as follows:

In chapter 2, we will state some basic definitions about discrete Morse theory and discrete bifurcation diagrams. In chapter 3, the definitions of persistence homology, stability of persistence diagrams and extended persistence homology are given. In the last chapter, we explain a method for drawing discrete bifurcation diagrams with the help of persistence diagrams. We use leukemic cells as data set to implement our method. At the end of the chapter 4, we compare our algorithm with the birth and death algorithm in [14].

CHAPTER 2

BACKGROUND

In this chapter, we will state some basic definitions about discrete Morse Theory and discrete bifurcation diagrams. One can find more details about them in [10], [11] and [14].

2.1 Discrete Morse Theory

Morse theory builds a bridge between the topology of a smooth manifold M and the critical points of a smooth function on M [17]. Recall that, for a real-valued smooth function f on a differentiable manifold M , the points where the differential of f vanishes are called critical points of f and their images under f are called critical values. If the Hessian matrix (the matrix of second partial derivatives) at a critical point P is non-singular, then P is called a non-degenerate critical point; if the Hessian is singular then P is called a degenerate critical point. A *Morse function* $f : M \rightarrow \mathbb{R}$ is a smooth function on a manifold M such that all critical points are non-degenerate and the critical values are distinct. Let us recall some basic definitions which are needed to describe discrete Morse theory.

Let $N = \{v_0, v_1, \dots, v_n\} \subset \mathbb{R}^d$. $x = \sum_{i=1}^n t_i v_i$ is an *affine combination* of the v_i if $\sum_{i=0}^n t_i = 1$. An affine combination, $x = \sum_{i=1}^n t_i v_i$ is a *convex combination* if all t_i are non-negative. The *convex hull* is the set of convex combinations. A *n-simplex* is the convex hull of $n + 1$ affinely independent points, denoted as $\sigma = \text{conv}\{v_i\}$, $i = 0 \dots n$. We say that v_i 's span σ and $\dim \sigma = n$. Briefly, a simplex of dimension $n \in \mathbb{N}$ is the convex hull of $n + 1$ points $v_i \in \mathbb{R}^d$, $i = 0, 1 \dots n$ consisting of point $x = \sum_{i=1}^n t_i v_i$, where $t_i \in \mathbb{R}_{\geq 0}$ and $\sum_{i=0}^n t_i = 1$. We give special names for dimensions,

0, 1, 2, 3. We call a 0-simplex as vertex, 1-simplex as edge, 2-simplex as triangle, and 3-simplex as tetrahedron.

Let σ be a n -simplex defined by the vertex set, $N = \{v_0, v_1, \dots, v_n\}$. A simplex τ defined by vertex set V such that $V \subseteq N$ is a *face* of σ denoted by $\tau \leq \sigma$, and σ is called as *coface* of τ denoted by $\sigma \geq \tau$. If $V \subset N$ then τ is called a *proper face* and denoted by $\tau < \sigma$.

A *geometric simplicial complex* is a finite set K of simplices satisfying that all faces of a simplex in K are in K and the intersection of two simplices in K is a face of both of them contained in K . The dimension of K is the maximum dimension of any of its simplices. The underlying space, $|K|$, is the union of its simplices together with the topology inherited from the Euclidean space in which the simplices live. A triangulation of a space X is a simplicial complex, K , whose underlying space is homeomorphic to X .

Besides the definition of a geometric simplicial complex there is an abstract version of it as follows:

An *abstract simplicial complex* A is a finite collection of sets α_i 's $i = 1, \dots, k$ such that if $\alpha_i \in A$ and $\beta \subseteq \alpha_i$ then $\beta = \alpha_j$ for some $j \in \{1, \dots, k\}$. The α_i 's are the simplices of A . The dimension of a simplex is $\dim(\alpha_i) = \text{card}(\alpha_i) - 1$ and the maximum dimension of any of its simplices gives the dimension of the complex A . A *face* of α_i is a non-empty subset $\beta \subseteq \alpha_i$, which is proper if $\beta \neq \alpha_i$. The vertex set is the union of all simplices, $\text{Vert}(A) = \cup \alpha_i$, the collection of all α_i 's such that $\alpha_i \in A$. A subcomplex is an abstract simplicial complex $B \subseteq A$. Two abstract simplicial complexes A and B are isomorphic if there is a bijection $b : \text{Vert}(A) \rightarrow \text{Vert}(B)$ such that $\alpha_i \in A$ iff $b(\alpha_i) \in B$. The largest abstract simplicial complex with a vertex set of size $n + 1$ is the n -dimensional simplex with a total number of faces. Given a (geometric) simplicial complex K , we can construct an abstract simplicial complex A by throwing away all simplices and retaining only their sets of vertices. We call A a *vertex scheme* of K . Symmetrically, we call K a geometric realization of A . Every abstract simplicial complex of dimension n has a geometric realization in \mathbb{R}^{2n+1} .

The main theorems of discrete Morse Theory are best stated in the language of CW-

complexes, so we continue with an overview of the basics of them.

Let B^n be the closed unit n -ball, $B^n = \{x \in \mathbb{R}^n : |x| \leq 1\}$. The boundary of B^n is the unit $(n - 1)$ -sphere $S^{n-1} = \{x \in \mathbb{R}^n : |x| = 1\}$. An n -cell σ denoted by σ^n is a topological space which is homeomorphic to B^n .

A finite *CW-complex* K is a topological space that can be written as:

$$K = \bigcup_n K^n$$

where K^n is obtained by attaching finitely many n -cells σ_α via the continuous attaching maps as seen in below:

$$h_\alpha : \partial\sigma_\alpha \approx S^{n-1} \rightarrow K^{n-1}.$$

Briefly,

$$K^n = K^{n-1} \amalg_\alpha \sigma_\alpha / a \sim h_\alpha(a), a \in \partial\sigma_\alpha.$$

A CW-complex is regular if attaching maps h_α are homeomorphisms onto their images.

Definition 2.1.1 ([10]). *A function $f : K \rightarrow \mathbb{R}$ is a discrete Morse function if for every p -cell $\sigma^p \in K$, the following two conditions hold:*

$$\begin{aligned} 1) l_1 &= \#\{\tau^{p+1} > \sigma^p \mid f(\tau^{p+1}) \leq f(\sigma^p)\} \leq 1 \\ 2) l_2 &= \#\{\nu^{p-1} < \sigma^p \mid f(\nu^{p-1}) \geq f(\sigma^p)\} \leq 1 \end{aligned}$$

That is, for any p -cell σ , there can be at most one $(p + 1)$ -cell τ containing p -cell σ such that $f(\tau^{p+1}) \leq f(\sigma^p)$. Similarly, there can be at most one $(p - 1)$ -cell ν contained in p -cell σ such that $f(\nu^{p-1}) \geq f(\sigma^p)$. By the definition, discrete Morse functions are functions on K that increase with the dimension of the cells; i.e., the values on all but at most one face of σ must be smaller than the value on σ itself.

Example 2.1.2. Let us consider the following example to illustrate the definition. Each vertices and edges have the function values on them. The function in figure

2.1 satisfies the definition 2.1.1, but the function in figure 2.2 is not a discrete Morse function, because the vertex $g^{-1}(5)$ violates the first condition, i.e., it has two higher dimensional neighbors on which g takes on lower values and the edge $g^{-1}(0)$ violates the second condition, i.e., it has two lower dimensional neighbors on which g takes on higher values.

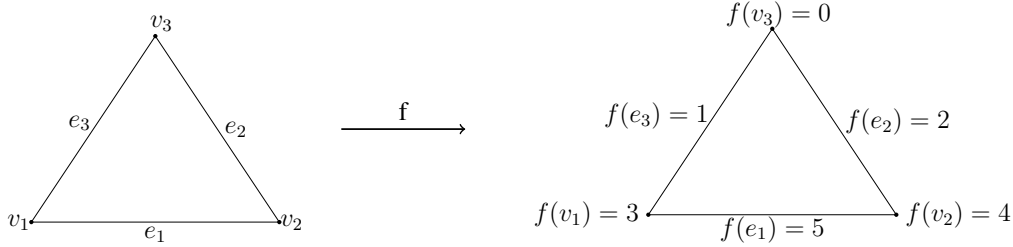


Figure 2.1: An example of a discrete Morse function

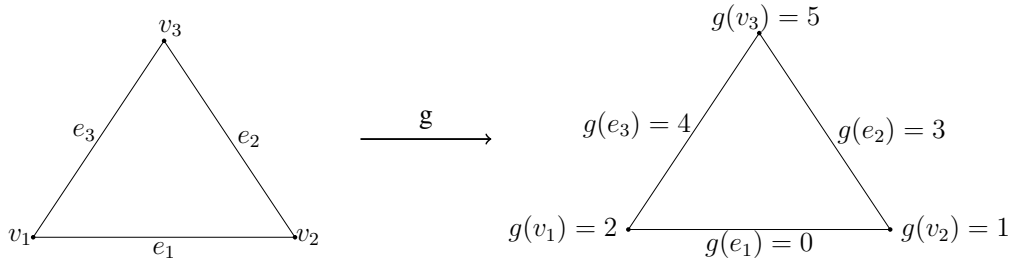


Figure 2.2: An example of a function which is not a discrete Morse function

Lemma 2.1.3 ([10]). *The numbers l_1 and l_2 in definition 2.1.1 cannot both be true.*

Proof. By the way of contradiction, let $l_1 = l_2 = 1$. Then there exist a $(p - 1)$ -cell ν and a $(p + 1)$ -cell β for a p -cell $\alpha \in K$ such that $f(\nu^{p-1}) \geq f(\alpha^p)$ and $f(\beta^{p+1}) \leq f(\alpha^p)$. Hence both inequalities give $f(\beta^{p+1}) \leq f(\alpha^p) \leq f(\nu^{p-1})$. Since K is a regular CW-complex, there is at least one p -cell $\tilde{\alpha}$ different from p -cell α , such that $\nu^{p-1} < \tilde{\alpha}^p < \beta^{p+1}$. Then $f(\nu^{p-1}) < f(\tilde{\alpha}^p)$ and $f(\tilde{\alpha}^p) < f(\beta^{p+1})$, so $f(\beta^{p+1}) \leq f(\alpha^p) \leq f(\nu^{p-1}) < f(\tilde{\alpha}^p) < f(\beta^{p+1})$ and this is a contradiction. \square

The other main subject in discrete Morse theory is the concept of a critical simplex.

Definition 2.1.4 ([10]). *A p -simplex σ^p is critical if*

- 1) $\#\{\tau^{p+1} > \sigma^p \mid f(\tau^{p+1}) \leq f(\sigma^p)\} = 0$,
- 2) $\#\{\nu^{p-1} < \sigma^p \mid f(\nu^{p-1}) \geq f(\sigma^p)\} = 0$.

Otherwise the simplex is called regular.

Note that every CW-complex K has a discrete Morse function. For example, if ν is a cell of K , we define $f : K \rightarrow \mathbb{R}$ by $f(\nu) = \dim(\nu)$. Hence every cell is critical.

If we consider the figure 2.1 in example 2.1.2, the edge $f^{-1}(5)$ and the vertex $f^{-1}(0)$ are critical simplices.

The following theorem is the main theorem of discrete Morse theory that determines the homotopy type of a complex. One can find more details in [10].

Theorem 2.1.5 ([10]). *Suppose K is a simplicial complex with a discrete Morse function. Then K is homotopy equivalent to a CW complex with exactly one cell of dimension p for each critical simplex of dimension p .*

Recall that in smooth Morse theory, one often works with the gradient vector fields of Morse functions rather than the function itself. There is a discrete version of this as follows:

For a discrete Morse function f on a simplicial complex K , we construct a vector field as follows: If α^p is a regular cell with β^{p+1} where $\beta^{p+1} > \alpha^p$ satisfying $f(\beta) \leq f(\alpha)$, then we draw an arrow from α to β . It can be seen that every simplicial complex satisfies one of the following properties: α is the tail of exactly one arrow, α is the head of exactly one arrow, α is neither the head nor the tail of an arrow. A cell α is critical if and only if it is neither the head nor the tail of an arrow.

The arrows that connect pairs of simplices arising from the discrete Morse function f on a simplicial complex K determine a discrete vector field called the *gradient vector field* of f .

Definition 2.1.6 ([10]). *Let K be a simplicial complex with a discrete Morse function f . A discrete vector field V on K is a collection of pairs $\{\alpha^p, \beta^{p+1}\}$ of simplices of K with $\alpha^p < \beta^{p+1}$ such that each simplex is at most one pair of V . The discrete gradient vector field of a discrete Morse function f on M consists of pairs $\{\alpha^p, \beta^{p+1}\}$ such that $\alpha > \beta$ and $f(\beta^{p+1}) \leq f(\alpha^p)$.*

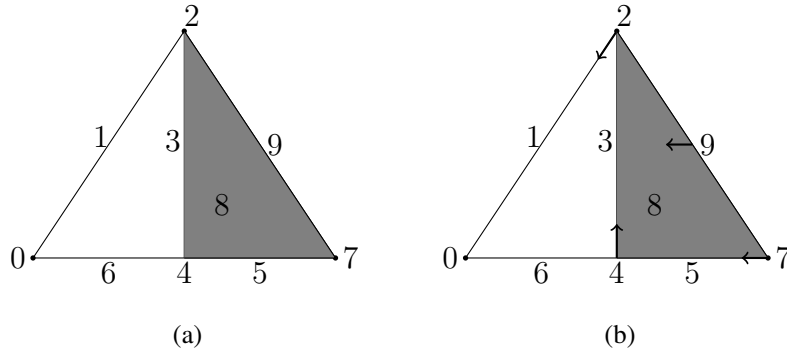


Figure 2.3: The vector field of (a) is in figure (b)

A collection of pairs $\{\alpha^p, \beta^{p+1}\}$ is in V if and only if $f(\beta^{p+1}) \leq f(\alpha^p)$. Briefly $\{\alpha^p, \beta^{p+1}\}$ is in V if and only if we draw an arrow from α to β where both of them form regular simplices. The arrow points from higher value to the lower value.

Example 2.1.7. The right triangle in figure 2.3 shows the arrows associated with the discrete Morse function from the left triangle. $f^{-1}(6)$ is a critical simplex of dimension 1 and $f^{-1}(0)$ is a 0-dimensional critical simplex. According to the theorem 2.1.5 the triangle is homotopic equivalent with a circle.

There are three types of critical simplices: a minimum, a saddle and a maximum. In figure 2.4, red dot is the minimum, yellow line is the saddle and pink triangle is the maximum critical simplex of dimension zero, one and two respectively according to the direction of vectors.

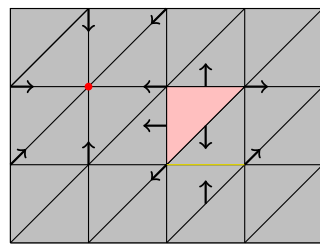


Figure 2.4: Minimum, saddle and maximum critical simplices

Definition 2.1.8 ([10]). Given a discrete vector field V on a simplicial complex K , a V -path is a sequence of simplices $\alpha_0^p, \beta_0^{p+1}, \alpha_1^p, \beta_1^{p+1}, \dots, \beta_s^{p+1}, \alpha_{s+1}^p$ such that for each $i=0, \dots, s$, $(\alpha < \beta) \in V$ and $\beta_i > \alpha_{i+1} \neq \alpha_i$. Such a path is a non-trivial closed path if $s \geq 0$ and $\alpha_0 = \alpha_{s+1}$.

Note that if V is the gradient vector field of a discrete Morse function f , then we call a V -path as a gradient path of f . We have the following result:

Theorem 2.1.9 ([10]). *Suppose V is the gradient vector field of a discrete Morse function f . Then a sequence of simplices as in definition 2.1.8 is a V -path if and only if $\alpha_i < \beta_i > \alpha_{i+1}$ for each $i = 0, 1, \dots, s$, and $f(\alpha_0) \geq f(\beta_0) > f(\alpha_1) \geq f(\beta_1) > \dots \geq f(\beta_s) > f(\alpha_{s+1})$.*

It means that the gradient paths of f are precisely those continuous sequences of simplices along which f is decreasing. In particular, this theorem implies that if V is a gradient vector field, then there are no nontrivial closed V -paths.

2.2 Bifurcation Diagram

In this section, we give definition and an example of bifurcation diagram of a Morse function. Then we will explain a discrete version of bifurcation diagram via birth and death algorithm in [14].

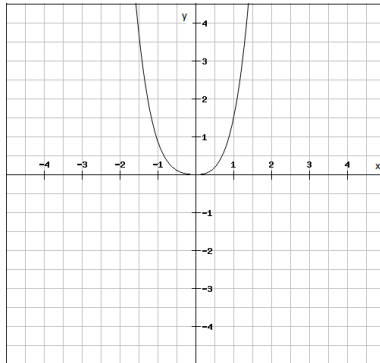
In dynamical systems, a bifurcation diagram shows the values visited or approached asymptotically like fixed points, periodic orbits, or chaotic attractors of a system as a function of a bifurcation parameter in the system.

Suppose that M is a smooth manifold and we have a family of functions $f : M \times I \rightarrow \mathbb{R}$ such that $f_t : M \rightarrow \mathbb{R}$ has only non-degenerate critical points for almost all t , that is f_t is generically Morse. As t changes, the critical points of f_t appear or disappear in M . If new critical points appear at time t_i we call that critical points are "born", if they disappear we say that they "die". Generically, critical points are born and die in pairs.

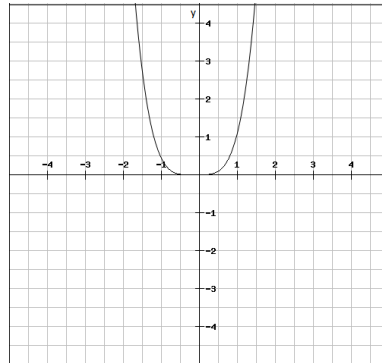
A bifurcation diagram is the graph of $f_x(x, t) = 0$ with x on the vertical axis and t on the horizontal axis where $x \in M$ and $t \in I$. Briefly, we can trace the critical points as t changes by the bifurcation diagram.

Now we will give a simple example which explains how to draw bifurcation diagram.

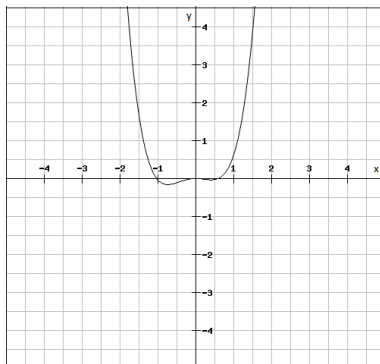
Example 2.2.1. Let $M=\mathbb{R}$ and consider $f : \mathbb{R} \times [-1, 1] \rightarrow \mathbb{R}$ defined by $f(x, t)=\frac{3x^4}{4} + \frac{x^3}{3} - \frac{tx^2}{2}$. For all t , $x = 0$ is a critical point. Other two critical points depend on t . f_t is Morse function except for when $t = 0$ and $x = 0$ is a degenerate critical point, and when $t = -1/24$, $x = -1/6$ is a degenerate critical point. We draw the following curves by using online program.



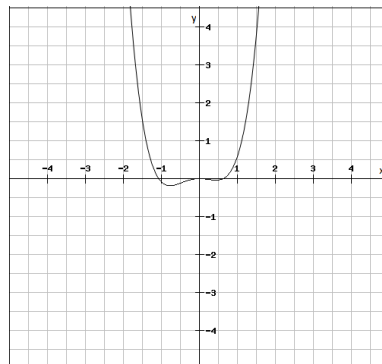
(a) The curve $f(x, t)$ for $t = -0.9$



(b) The curve $f(x, t)$ for $t = -0.04$



(c) The curve $f(x, t)$ for $t = 0.9$



(d) The curve $f(x, t)$ for $t = 1$

Figure 2.5: The curves $f(x, t)$ for $t = -0.9, -0.04, 0.9, 1$

The graph of $t = 3x^2 + x$ is the bifurcation diagram as seen in figure 2.6.

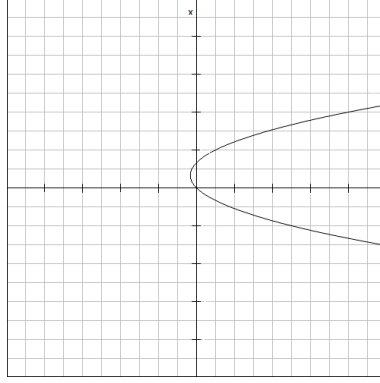


Figure 2.6: Bifurcation diagram of $f(x, t) = \frac{3x^4}{4} + \frac{x^3}{3} - \frac{tx^2}{2}$

2.2.1 Discrete Bifurcation Diagram

Let K be a finite simplicial complex and suppose that for each $0=t_0, t_1, \dots, t_r = 1$, we have a discrete Morse function $f_{t_i} : K \rightarrow \mathbb{R}$ defined on K for each i . The simplicial complex $K_i = K \times \{t_i\} \subset K \times I$ is called a *slice*. A *discrete bifurcation diagram* is a diagram which shows whether or not the critical cells in each slice live in the adjacent slices or a new critical cell appear in the next slice.

Now we are going to overview the method given in [15] for sketching discrete bifurcation diagram by using the birth and death algorithm [14]. In applications, the values of each f_{t_i} would be given only on vertices in K , then this function can be extended to a discrete Morse function on all of K via the *Morse* algorithm in [15].

Let K be a simplicial complex and v be a vertex of K . The *star* of v , denoted by $St(v)$, is the minimal subcomplex of K which contains all the simplices that contain v .

The *link* of v , denoted by $Lk(v)$, is the subcomplex of $St(v)$ which contains all the simplices that do not contain v . The *lower link* of v denoted as $Lk_-(v)$ contains all the simplices of the link that have lower value of discrete Morse function on all its vertices.

For disjoint simplices $\alpha_1, \alpha_2 \in K$, $\alpha_1 * \alpha_2$ is a notation for joining them. It is either a simplex of K that has the union of vertices of α_1 and α_2 or if this simplex does not exist in K then it is undefined.

The input of this algorithm is a finite simplicial complex K , an injective function $j : Vert(K) \rightarrow \mathbb{R}$, where $Vert(K)$ is the set of vertices of K and its output is sets A , B and C of simplices of K and a bijective map $l : B \rightarrow A$ such that $l(\alpha)$ is a co-dimension one face of $\alpha \in B$. The map l defines which simplices are paired. The set C consists of critical simplices. The algorithm finds the lower link of vertices to determine the sets A , B , and C . The outline of this algorithm is as follows:

- Set A , B , C to be empty.
- foreach $v \in Vert(K)$
 - let K' be the lower link of v
 - if K' is empty then add v to critical set C .
 - else
 - add v to the set A
 - let $j' : vert(K') \rightarrow \mathbb{R}$ be the restriction of j
 - let A', B', C', l' denote the resulting partition of the simplices of K' ;
 - find $w_0 \in C'_0$ so that $j'(w_0)$ is the smallest; add $[v, w_0]$ to B , set $l([v, w_0]) = v$;
 - for each $\alpha \in C' - w_0$ add $v * \alpha$ to C ;
 - for each $\alpha \in B'$ add $v * \alpha$ to B , add $v * l'(\alpha)$ to A , and set $l(v * \alpha) = v * l'(\alpha)$.
 - end if
- continue foreach

This algorithm produces large set of critical simplices. In order to decrease the number of them, the direction of arrows in the gradient path is reversed, so that, critical simplices are paired and they are not critical any more. One of the important results of this algorithm is that it does not produce directed loops if there is only one gradient path between them. The following simple example illustrates the above algorithm.

Example 2.2.2. Let K be a figure with the function $h : Vert(K) \rightarrow \mathbb{R}$ given as in figure 2.7. Each vertex is denoted by its h -value.

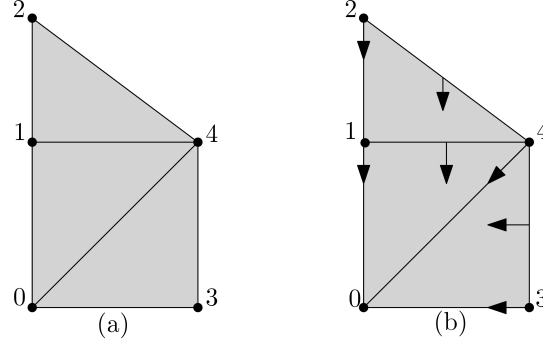


Figure 2.7: Gradient vector field

The algorithm is proceeded through the vertices of K beginning at 0. Implementing the algorithm gives the following.

$$0 : A = \emptyset, B = \emptyset, C = \{0\}$$

$$1 : A = \{1\}, B = \{[1, 0]\}, C = \{0\}$$

$$2 : A = \{1, 2\}, B = \{[1, 0], [2, 1]\}, C = \{0\}$$

$$3 : A = \{1, 2, 3\}, B = \{[1, 0], [2, 1], [3, 0]\}, C = \{0\}$$

$$4 : A = \{1, 2, 3, 4, [4, 1], [4, 2], [4, 3]\},$$

$$B = \{[1, 0], [2, 1], [3, 0], [4, 0], [4, 1, 0], [4, 2, 1], [4, 3, 0]\}, C = \{0\}.$$

The discrete vector field of figure 2.7 (a) is in figure 2.7 (b).

Now we briefly explain birth and death algorithm. In this algorithm, there are two cases to consider. In the first one, the triangulations in each slice are same and in the second case the triangulations are different on each slice.

Definition 2.2.3 ([14]). *Suppose α and β are k -cells in K and α is critical for V_i and β is critical for V_j . If there is a k -cell λ and a V_i path α, \dots, λ of k - and $(k - 1)$ -cells and a V_j path λ, \dots, β of k - and $(k + 1)$ -cells, then α is connected to β . The critical cell α is strongly connected to β if α is connected to β and β is connected to α .*

Strong connectivity between critical cells in a discrete bifurcation diagram gives a way to follow the births and deaths of critical cells. If there is no strong connectivity between a critical cell α for V_i and any critical cell for V_{i+1} , then we say that the critical cell α dies. If a critical cell α for V_i is not strongly connected to any critical cell for V_{i-1} then it is born. If a critical cell α for V_i is strongly connected to exactly one cell β for V_{i+1} and β is not strongly connected to any other critical cell for V_i then α moves to β .

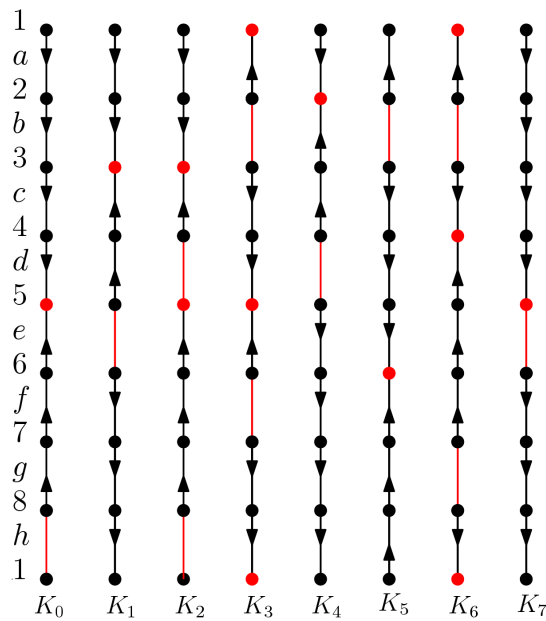


Figure 2.8: A family of discrete gradient fields on the circle.

Example 2.2.4. Figure 2.8 shows of a family of discrete gradient vector fields on the circle. The slices are numbered from 0 to 7. The connectivity diagrams for the 0- and 1-cells are shown in figure 2.9. In this figure the black lines show the strong connections, while the red lines indicate connections in one direction only in adjacent slices. There are following births: vertex 5 in slice 2, vertex 1 in slice 3, and vertex 1 in slice 6; edge d in slice 2, edge b in slice 3, and edge g in slice 6. The deaths are: vertex 3 in slice 2, vertex 5 in slice 3, and vertex 1 in slice 6; edge e in slice 1, edge d in slice 2, and edge f in slice 3.

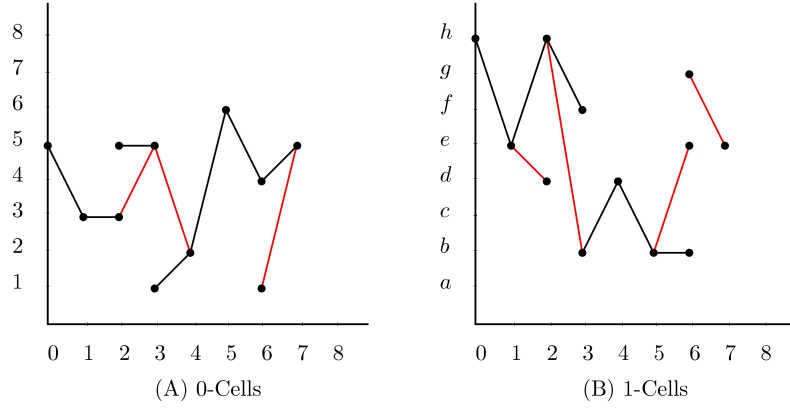


Figure 2.9: The connectivity diagrams associated with the example in Figure 2.8

In the second case, firstly a refinement of discrete vector field is done, then the algorithm in the first case is applied.

A cell complex N is a refinement of a cell complex K if each cell of N is contained in some cell of K . For example, a barycentric subdivision of a simplicial complex is a refinement.

Definition 2.2.5 ([14], Refinement of discrete vector fields). *Let V be a discrete vector field on a cell complex K and let N be a refinement of K . If τ is a cell of N let $g(\tau)$ be the smallest dimensional cell of K so that τ is contained in $g(\tau)$. A discrete vector field W on N is a refinement of V if for each m -cell β of K we can find a m -cell $h(\beta)$ of N so that:*

- (1) $h(\beta) \subset \beta$.
- (2) If β is critical then $h(\beta)$ is critical.
- (3) If $(\beta, \alpha) \in V$ then $(h(\beta), h(\alpha)) \in W$
- (4) If $(\kappa, \tau) \in W$ and $\kappa \neq h \circ g(\kappa)$ then $g(\kappa) = g(\tau)$.

For the cell complexes K and a refinement N there exists a refinement W of V with no additional critical cells. We may obtain N from K by the following subdivisions:

- (1) adding a new vertex in the interior of a cell and subdividing the cell into cones to the boundary cells,
- (2) dividing a cell along a sphere of co-dimension 1 which forms a sub-complex

in its boundary into three new cells, and the boundary sphere of each cell admits a discrete vector field with the minimal number of critical cells.

An example of a refinement of a discrete vector field is shown in (b) of figure 2.10. A new vertex is added in the interior of triangle and the cell is subdivided into cones to the boundary cells. Note that α , e and v are the critical cells. Then $h(\alpha)$, $h(e)$ and $h(v)$ are the critical cells of the refined discrete vector fields.

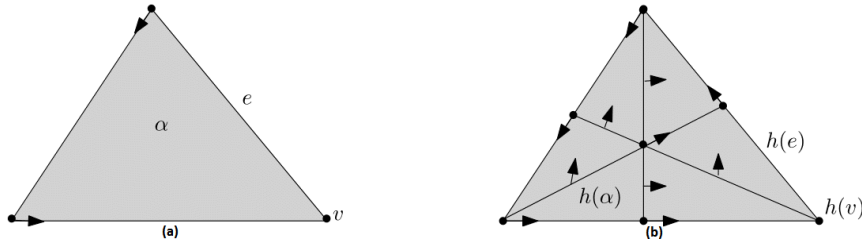


Figure 2.10: (b) is the refinement of (a)

King et.al. [14] consider the common subdivision of slices K_i and K_{i-1} and call it as $K_{i-1/2}$. They set V_i^- is a refinement of V_i on $K_{i-1/2}$ with respect to the choice $h : K_i \rightarrow K_{i-1/2}$. Then a critical cell α^k in K_i is connected to a critical cell β^k in K_{i-1} if there exists a cell γ^k in $K_{i-1/2}$ which is connected to $h_i(\alpha)$ along a path in V_i^- and to β along a path in V_{i-1} . This can be done backwards, from K_{i-1} to K_i .

Example 2.2.6. [14] The connectivity diagrams associated with this example are in figure 2.12 which give the discrete bifurcation diagram for the different triangulations.

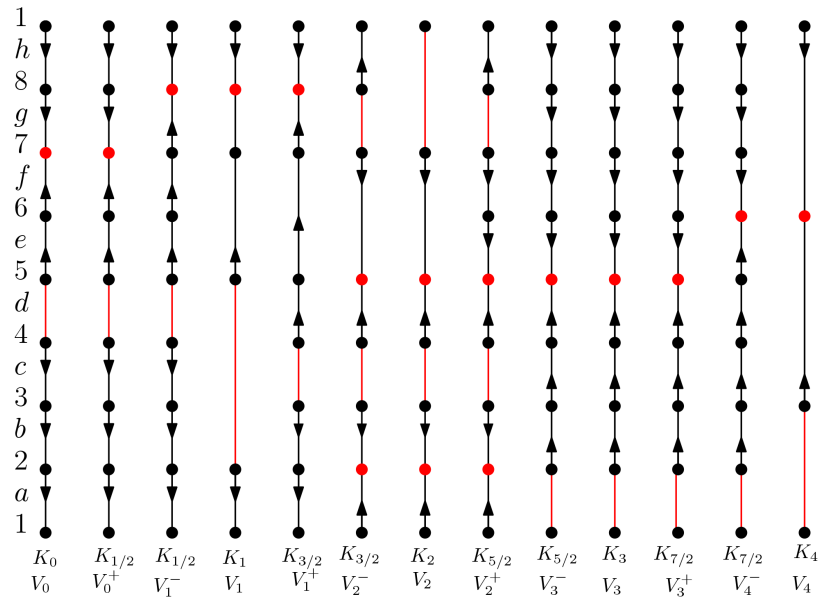


Figure 2.11: A family of discrete gradient fields on the circle with different triangulations.

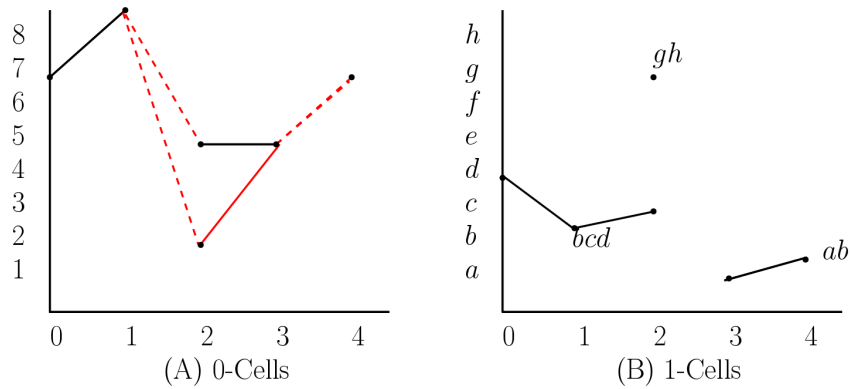


Figure 2.12: The connectivity diagrams associated with the example 2.2.6

CHAPTER 3

PERSISTENCE HOMOLOGY

In this chapter, we will give some basic definitions about persistence homology, then we will explain stability of persistence diagrams and extended persistence homology. This section is based on [7], [4], [5].

3.1 Basic Definitions

Persistence homology is a tool used for the measurement of topology of a shape. To define persistence homology we need a nested sequence of space $\{X_r\}_{r \in \mathbb{R}}$ such that $X_a \subset X_b$ if $a \leq b$, called *filtration*. There are several types of filtration. One of them is the sublevel set. Let us recall it as follows:

Definition 3.1.1. Let $f : X \rightarrow \mathbb{R}$ be a monotonic function on a simplicial complex X , i.e. $f(\tau) \leq f(\sigma)$ if τ is a face of σ . Let $-\infty = a_0 \leq a_1 \leq a_2 \leq \dots \leq a_n$ be the function values of the simplices in X . The sublevel set $X_i = f^{-1}(-\infty, a_i]$, is a subcomplex of X for every $a_i \in \mathbb{R}$.

Example 3.1.2. Let f be a discrete Morse function on simplicial complex X with 4 edges and 4 vertices. The sublevel set is then as in figure 3.1.

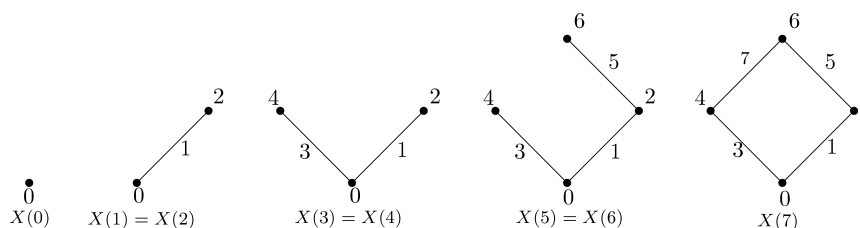


Figure 3.1: The sublevel set

Let us recall a standard result from algebraic topology.

Lemma 3.1.3 ([19], Induced homomorphism). *Let A, X be two simplicial complexes with $A \subseteq X$. Then the inclusion map $i : A \hookrightarrow X$ induces a homomorphism $H_p(A) \rightarrow H_p(X)$ for each dimension p .*

The filtration and lemma 3.1.3 give a sequence of homology groups which enables us observing the topological changes. For every $i \leq j$ there is an inclusion map from X_i to X_j and that induces a homomorphism,

$$f_q^{i,j} : H_q(X_i) \rightarrow H_q(X_j)$$

for each dimension q . Then we have a sequence of homomorphisms induced by inclusions.

$$0 = H_q(X_0) \rightarrow H_q(X_1) \rightarrow H_q(X_2) \rightarrow \dots \rightarrow H_q(X_n) = H_q(X)$$

for each dimension q .

Definition 3.1.4. *The q -th persistent homology groups are the images of $f_q^{i,j}$, denoted by $H_q^{i,j} = \text{im}(f_q^{i,j})$, for $0 \leq i \leq j \leq n$. The rank of image is called the q -th persistent Betti number and denoted by $\beta_q^{i,j} = \text{rank}(\text{im}(f_q^{i,j}))$.*

The persistent homology groups consist of the homology classes of X_i that are still living in X_j , that is,

$$H_q^{i,j} = Z_q(X_i) / (B_q(X_j) \cap Z_q(X_i)).$$

A homology class $\xi \in H_q(X_i)$ is said to be "born" at X_i if $\xi \notin H_q^{i-1,i}$. A homology class ξ born at X_i is said to "die" entering X_j where $j > i$, if it merges with an older class while proceeding from X_{j-1} to X_j , i.e., $f_q^{i,j-1}(\xi) \notin H_q^{i-1,j-1}$, but $f_q^{i,j}(\xi) \in H_q^{i-1,j}$. See figure 3.2. If at X_j two classes merge, the older one remains and the younger one ends. This is called as *Elder Rule*.

Definition 3.1.5. *If ξ is born at X_i and dies entering X_j then the persistence of a class is $\text{pers}(\xi) = (a_j - a_i)$ where ξ is born at the function value a_i and dies at the function value a_j . If ξ is born at X_i but never dies, then its persistence is infinity. Sometimes the difference in index, $j - i$ is considered and is called as index persistence of the class.*

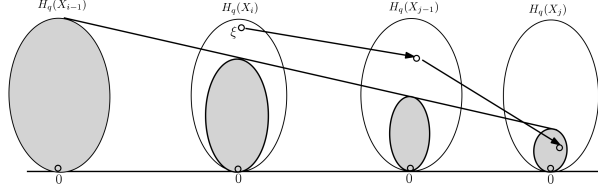


Figure 3.2: The class ξ born at X_i since it does not lie in the (gray) image of H_q^{i-1} . The class ξ dies entering X_j since this is the first time its image merges into the image of H_q^{i-1} .

Definition 3.1.6. Given a filtration $\emptyset = X_0 \subset X_1 \subset \dots \subset X_u = X$. We call q -simplex τ as positive (a class borns) if it is added at X_i and creates a cycle. If q -simplex σ enters at X_j and fills in a cycle then we call it as negative simplex (a class dies).

Definition 3.1.7. A negative simplex is paired with a youngest positive simplex through the elder rule. This is called "persistence pairs".

Definition 3.1.8. The number of q -dimensional classes born at X_i and die at X_j is called multiplicity denoted by $\mu_q^{i,j}$ and is computed as:

$$\mu_q^{i,j} = (\beta_q^{i,j-1} - \beta_q^{i-1,j-1}) - (\beta_q^{i,j} - \beta_q^{i-1,j})$$

for all q and $i < j$.

For a homology class ξ with index persistence $j - i$, we draw a point on the plane with coordinate (i, j) where the distance of the point to the diagonal is the persistence of the class.

Definition 3.1.9. A diagram in which each point (i, j) is drawn with multiplicity $\mu_q^{i,j}$ on the extended plane $\overline{\mathbb{R}^2}$ ($\overline{\mathbb{R}} = \mathbb{R} \cup \{-\infty, \infty\}$) where the x -axis represents the birth and y -axis represents the death and the diagonal is added with infinite multiplicity is called the q -th persistence diagram and denoted by $Dgm_q(f)$.

Persistence diagrams are multi set because classes can be born at some time and they can die at some time. Some of the classes may never die and are represented as points at infinity. Since $\mu_q^{i,j}$ is defined for $i < j$, (i, j) lies above the diagonal. Note that $\beta_q^{i,j}$ is the number of points lie in the left upper corner of the point (i, j) .

Definition 3.1.10. For every pair of indices $0 \leq t \leq u \leq w$ and every dimension q , the q -th persistent Betti number is $\beta_q^{t,u} = \sum_{i \leq t} \sum_{j > u} \mu_q^{i,j}$.

Example 3.1.11. This example finds the number of cycles born in X_1 and die in X_3

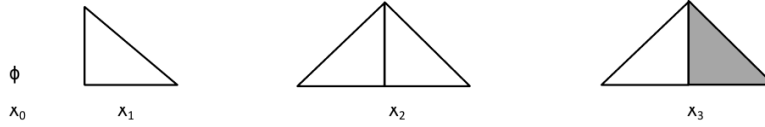


Figure 3.3: Filtration

$$\beta_1(X_1) = 1, \quad \beta_1(X_2) = 2, \quad \beta_1(X_3) = 1.$$

The first persistent Betti numbers are: $\beta_1^{1,2} = 1$, $\beta_1^{1,3} = 0$, $\beta_1^{2,3} = 1$.

$$\begin{aligned} \mu_1^{1,3} &= (\beta_1^{1,2} - \beta_1^{0,2}) - (\beta_1^{1,3} - \beta_1^{0,3}) \\ &= (1 - 0) - (0 - 0) \\ &= 1 \end{aligned}$$

Example 3.1.12.

Let X be simplicial complex with function values on it. The sublevel set according to the function values is seen in figure 3.4.

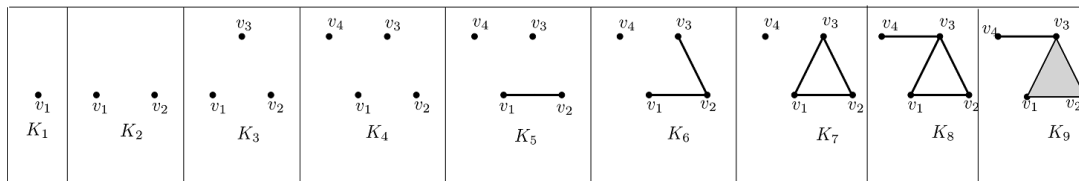


Figure 3.4: The sublevel set

The vertex v_2 borns as a 0-cycle in filtration K_2 and dies when the edge $[v_1, v_2]$ is added in filtration K_5 . Similarly, the vertex v_3 borns as a 0-cycle in filtration K_3 and it dies in K_6 . Adding the edge $[v_1, v_3]$ in K_7 does not kill anything, since it creates a 1-cycle. This 1-cycle is killed by the triangle in K_9 . The zeroth and the first persistence diagram from left to right are then shown in figure 3.5.

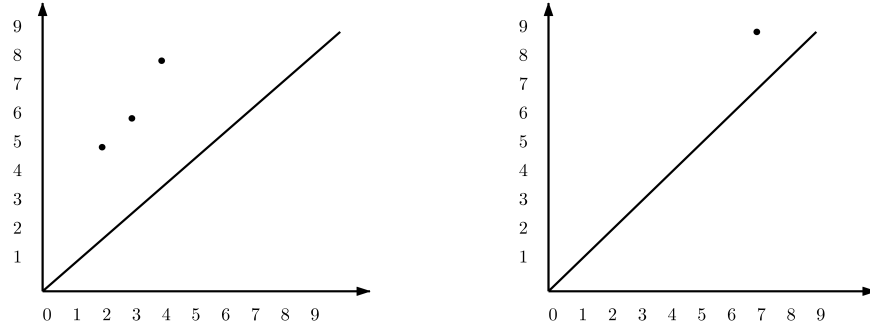


Figure 3.5: Persistence diagrams of figure 3.4

Matrix reduction is another algorithm to compute persistence. We use a filtration of a simplicial complex, $\emptyset = X_0 \subset X_1 \subset \dots \subset X_n = X$ and compatible total ordering of the simplices, $\tau_1, \tau_2, \dots, \tau_m$ in X , that is ; the simplices in each complex X_m in the filtration precede the ones in $X - X_m$ and the faces of a simplex precede the simplex. The boundary matrix denoted by ∂ is found as follows:

$$\partial[k, l] = \begin{cases} 1 & \text{if } \tau_k \text{ codimension one face of } \tau_l \\ 0 & \text{if not} \end{cases} \quad (3.1)$$

Let $low(j)$ be the row index of the lowest 1 in column j . We use column operations from left to right to put ∂ in a form if $low(j) \neq low(k)$ whenever $j \neq k$. This form is called reduced matrix and denoted by R . To get the ranks of the homology groups of K , we denote the zero columns that correspond to q -simplices by $\#Zero_q(R)$ and we denote the lowest ones in rows that correspond to q -simplices by $\#Low_q(R)$. If we compare the reduced matrix with the normal form matrices, we have $\#Zero_q(R) = rank Z_p$ and $\#Low_q(R) = rank B_q$. It follows that $\beta_q = rank Z_p - rank B_q \forall q$.

Proposition 1 ([9]). Let $R = \partial V$, where R is in reduced form and V is upper triangular. Then, the simplices τ_k and τ_l form a persistent pair if and only if $low(l) = k$.

Note that if column j of R is zero then τ_j is positive, that is, its addition creates a new cycle and gives birth to a new homology class and it does not get paired with a negative simplex.

Example 3.1.13.

Let X be simplicial complex with filtration as in figure 3.4. The boundary matrix is in figure 3.6 where gray colour indicates that the matrix entry is 1.

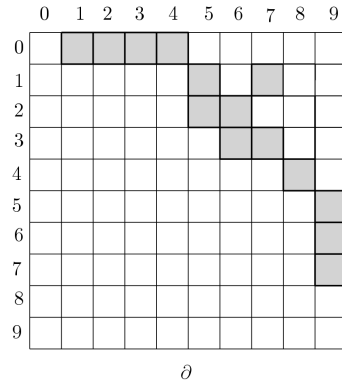


Figure 3.6: The boundary matrix

The column operation on boundary matrix from left to right results in a reduced matrix as in figure 3.7. There are five non zero columns. The $low(j)$ is coloured with dark gray. For instance $low(5)$ is 2 which means that the vertex v_2 borns as a 0-cycle in filtration K_2 and dies when the edge $[v_1, v_2]$ is added in filtration K_5 . Similarly, the vertex v_3 borns as a 0-cycle in filtration K_3 and it dies in K_6 . Since the column 7 is zero, adding the edge $[v_1, v_3]$ in K_7 does not kill anything in fact it creates a 1-cycle. This 1-cycle is killed by the triangle in K_9 . We obtain the same zeroth and first persistence diagram as in figure 3.5.

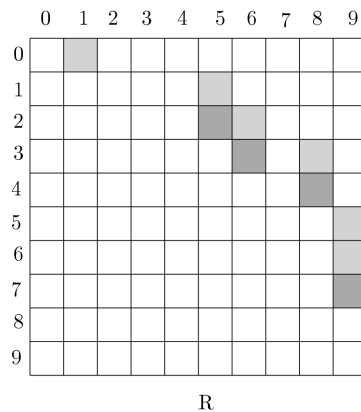


Figure 3.7: Reduced boundary matrix

3.2 Stability of Persistence Diagrams

Persistence is a way of measuring data. If a small perturbation in the data gives small changes in persistence, then this implies that our way of measurement is stable. In this section we will make this statement precise.

In this section we use the following short notation. Let X be a topological space and $f : X \rightarrow \mathbb{R}$. For fixed $i \in \mathbb{Z}$ let $F_x = H_i(f^{-1}(-\infty, x])$, and for $x < y$ we have $f^{-1}(-\infty, x] \subset f^{-1}(-\infty, y]$ and let $f_x^y : F_x \rightarrow F_y$ be a map induced by inclusion of the sublevel set. The $\text{Im} f_x^y$ is shortly denoted by F_x^y . Recall from the previous section that the dimension of F_x^y is the persistent Betti number and it will be denoted by β_x^y . We set $F_x^y = 0$ when x or y is infinite. We will work with modulo 2 coefficients, so that homology groups are vector spaces over the field \mathbb{Z}_2 .

Definition 3.2.1 ([4]). *Let X be a topological space and f be a real valued function on X . A homological critical value of f is a real number c , for which there exists an integer i such that for all sufficiently small $\epsilon \geq 0$ the map induced by inclusion $H_i(f^{-1}(-\infty, c - \epsilon]) \rightarrow H_i(f^{-1}(-\infty, c + \epsilon])$ is not an isomorphism.*

It means that, the homological critical values are the levels where the homology of the sublevel sets changes. For a Morse function f , the Morse theory gives that its homological critical values coincide with its classical critical values.

Definition 3.2.2 ([4]). *A function $f : X \rightarrow \mathbb{R}$ is tame function if it has a finite number of homological critical values and the homology groups $H_i(f^{-1}(-\infty, c])$ are finite dimensional $\forall i \in \mathbb{Z}$ and $c \in \mathbb{R}$.*

The following lemma is concluded from definition 3.2.1.

Lemma 3.2.3 ([4]). *If some closed interval $[a, b]$ contains no homological critical value of f , then f_a^b is an isomorphism.*

Proof. Let $n = (a + b)/2$, we have $a < n < b$. For $a < n$, $f^{-1}(-\infty, a] \subset f^{-1}(-\infty, n]$ and for $n < b$, $f^{-1}(-\infty, n] \subset f^{-1}(-\infty, b]$. We have $f_a^b = f_n^b \circ f_a^n$. If f_a^b is not isomorphism, then one of f_a^n and f_n^b is not isomorphism. By induction,

there is a decreasing sequence of intervals whose intersection is a homological critical value in $[a, b]$, and this contradicts with the assumption. \square

We denote Δ for the diagonal entries of the persistence diagram. $\#(Dgm_q(f) - \Delta) = \sum_{r < s} \mu_q^{r,s}$ is the total multiplicity of a multi set $(Dgm_q(f) - \Delta)$ which is the sum of multiplicities of the elements in $Dgm_q(f) - \Delta$. This number gives the size of the persistence diagram.

Lemma 3.2.4 gives us a relation between total multiplicity of persistence diagrams and Betti numbers. We use $Q_a^b = [-\infty, a] \times [b, \infty]$ to denote the closed upper left quadrant with corner (a, b) .

Lemma 3.2.4 ([4]). *Let f be a tame function and suppose $a < b$ are different from the homological critical values of f . Then the total multiplicity of the persistence diagram within the upper left quadrant is $\#(Dgm_q(f) \cap Q_a^b) = \beta_a^b$.*

Proof. Let $a = b_i$ and $b = b_{j-1}$. The total multiplicity in the upper left quadrant is

$$\begin{aligned} \mu &= \sum_{r \leq i \leq j \leq s} \mu_r^s \\ &= \sum_{r \leq i \leq j \leq s} (\beta_{b_{r-1}}^{b_s} - \beta_{b_r}^{b_s} + \beta_{b_r}^{b_{s-1}} - \beta_{b_{r-1}}^{b_{s-1}}) \\ &= \beta_{b_{-1}}^{b_{n+1}} - \beta_{b_i}^{b_{n+1}} + \beta_{b_i}^{b_{j-1}} - \beta_{b_{-1}}^{b_{j-1}} \end{aligned}$$

Except for $\beta_{b_i}^{b_{j-1}}$ which is β_a^b , all other terms vanish. \square

To make stability precise we need two notions of distance called as Hausdorff and bottleneck distance.

For points $a = (a_1, a_2)$ and $b = (b_1, b_2)$ in $\overline{\mathbb{R}}^2$, let $\|a - b\|_\infty = \max\{|a_1 - b_1|, |a_2 - b_2|\}$. For functions f and g , let $\|f - g\|_\infty = \sup_{x \in X} |f(x) - g(x)|$.

Definition 3.2.5. *Let X and Y be multisets of points in $\overline{\mathbb{R}}^2$. The Hausdorff distance is*

$$d_H(X, Y) = \max\{\sup_{x \in X} \inf_{y \in Y} \|x - y\|_\infty, \sup_{y \in Y} \inf_{x \in X} \|y - x\|_\infty\}$$

The bottleneck distance is

$$d_B(X, Y) = \inf_{\rho} \sup_{x \in X} \|x - \rho(x)\|_{\infty}$$

where ρ ranges over all bijections from X to Y .

In words, to find the bottleneck distance we consider all bijections $\rho: X \rightarrow Y$ and find the largest distances between corresponding points for each bijection and take the infimum of these largest values.

In our case we use persistence diagrams as multi sets of points. If the two diagrams do not have the same number of points, we are allowed to borrow points from the horizontal axis to form bijections.

Let X and Y be two persistence diagrams. A bijection from X to Y can take an off diagonal point to an off diagonal point, an off diagonal point to a diagonal point, or a diagonal point to a diagonal point. The most important one is the first one. The least one is the third one.

Since the bottleneck distance between $Dgm(f)$ and $Dgm(g)$ is the infimum, over all bijections $\rho : Dgm(f) \rightarrow Dgm(g)$, of the largest distance between corresponding points and Hausdorff distance finds the maximum distance of a multiple set to the nearest point in the other multiple set then $d_H(X, Y) \leq d_B(X, Y)$.

Theorem 3.2.6 ([4]). *Let X be a triangulable space with continuous tame functions $f, g : X \rightarrow \mathbb{R}$. Then the persistence diagrams gives $d_B(Dgm_q(f), Dgm_q(g)) \leq \|f - g\|_{\infty}$.*

This theorem is called as Bottleneck Stability Theorem for persistence diagrams. It says that if a small perturbation in the data gives small changes in persistence, then this implies that our way of measurement is stable.

In figure 3.8, we have two close functions. The function g has many and the function f has two critical values. The corresponding persistence diagrams of both of them is on the right.

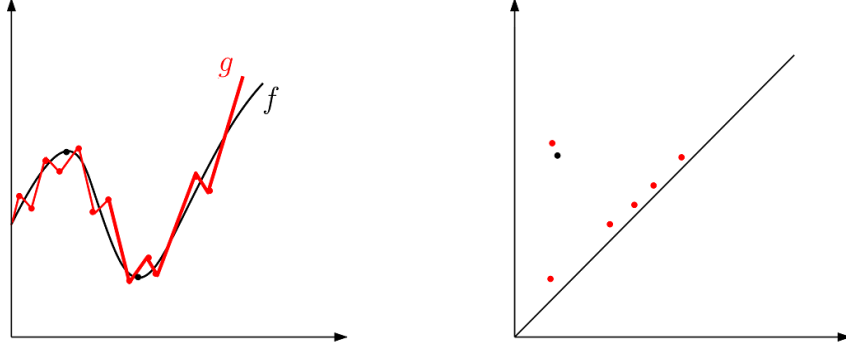


Figure 3.8: Close functions and persistence diagram

If the bottleneck stability theorem for persistence diagrams holds since

$$d_H(Dgm_q(f), Dgm_q(g)) \leq d_B(Dgm_q(f), Dgm_q(g))$$

then we have $d_H(Dgm_q(f), Dgm_q(g)) \leq \|f - g\|_\infty$ which is called as Hausdorff stability for persistence diagrams.

Theorem 3.2.6 is proved in two steps. First the stability of persistence diagrams for the Hausdorff distance will be shown and by using the Hausdorff stability of persistence diagrams we will show the bottleneck stability.

For $x < y$ we have $f^{-1}(-\infty, x] \subset f^{-1}(-\infty, y]$ and let $f_x^y : F_x \rightarrow F_y$ be a map induced by inclusion of the sublevel set.

Let f and g be two tame functions on a topological space X . For all $a \in \mathbb{R}$, let $F_a = H_i(f^{-1}(-\infty, a])$ and $G_a = H_i(g^{-1}(-\infty, a])$. For $a < b$, $f^{-1}(-\infty, a] \subset f^{-1}(-\infty, b]$ and let $f_a^b : F_a \rightarrow F_b$ be map induced by inclusion. Similarly for $a < b$, $g^{-1}(-\infty, a] \subset g^{-1}(-\infty, b]$ and let $g_a^b : G_a \rightarrow G_b$ be map induced by this inclusion. We use F_a^b for $im f_a^b$ and G_a^b for $im g_a^b$.

If $\|f - g\|_\infty = \epsilon$, then $f^{-1}(-\infty, a] \subseteq g^{-1}(-\infty, a + \epsilon] \forall a \in \mathbb{R}$. To show this inclusion, let us take $x \in f^{-1}(-\infty, a]$ then we have $f(x) \leq a$. $\|f - g\|_\infty = \sup_{x \in X} |f(x) - g(x)| = \epsilon$. $|f(x) - g(x)| \leq \epsilon$ which implies $-\epsilon \leq g(x) - f(x) \leq \epsilon$. So we get $g(x) \leq f(x) + \epsilon \leq a + \epsilon$. Therefore $x \in g^{-1}(-\infty, a + \epsilon]$. Now consider $\rho_a : F_a \rightarrow G_{a+\epsilon}$ induced by the above inclusion. Similarly we have $g^{-1}(-\infty, a] \subseteq f^{-1}(-\infty, a + \epsilon] \forall a \in \mathbb{R}$ which induces a map $\phi_a : G_a \rightarrow F_{a+\epsilon}$.

Let $a < b$, we have the following commutative diagram since each map is an inclusion.

$$\begin{array}{ccc}
f^{-1}(-\infty, a - \epsilon] & \hookrightarrow & f^{-1}(-\infty, b + \epsilon] \\
\downarrow & & \uparrow \\
g^{-1}(-\infty, a] & \hookrightarrow & g^{-1}(-\infty, b] \\
f^{-1}(-\infty, a + \epsilon] & \hookrightarrow & f^{-1}(-\infty, b + \epsilon] \\
\uparrow & & \uparrow \\
g^{-1}(-\infty, a] & \hookrightarrow & g^{-1}(-\infty, b]
\end{array}$$

These inclusion maps induce the following commutative diagrams.

$$\begin{array}{ccc}
F_{a-\epsilon} & \xrightarrow{f_{a-\epsilon}^{b+\epsilon}} & F_{b+\epsilon} \\
\downarrow \rho_{a-\epsilon} & & \uparrow \phi_b \\
G_a & \xrightarrow{g_a^b} & G_b
\end{array}
\quad
\begin{array}{ccc}
F_{a+\epsilon} & \xrightarrow{f_{a+\epsilon}^{b+\epsilon}} & F_{b+\epsilon} \\
\uparrow \phi_a & & \uparrow \phi_b \\
G_a & \xrightarrow{g_a^b} & G_a^b
\end{array}$$

By commutativity of the left diagram, we have $f_{a-\epsilon}^{b+\epsilon} = \phi_b \circ g_a^b \circ \rho_{a-\epsilon}$. Let $\zeta \in F_{a-\epsilon}^{b+\epsilon}$, then there exists $\xi \in F_{a-\epsilon}$ such that $\zeta = f_{a-\epsilon}^{b+\epsilon}(\xi)$. Therefore $\zeta = \phi_b(\eta)$ where $\eta = g_a^b(\rho_{a-\epsilon}(\xi))$, that is $\eta \in G_a^b$. Hence we have $F_{a-\epsilon}^{b+\epsilon} \subseteq \phi_b(G_a^b)$. Considering the diagram on the right, we have $\phi_b(G_a^b) = \phi_b \circ g_a^b(G_a)$. This implies that $f_{a+\epsilon}^{b+\epsilon} \circ \phi_a(G_a) \subseteq F_{a+\epsilon}^{b+\epsilon}$. Finally we have

$$F_{a-\epsilon}^{b+\epsilon} \subseteq \phi_b(G_a^b) \subseteq F_{a+\epsilon}^{b+\epsilon}$$

Therefore $\dim F_{a-\epsilon}^{b+\epsilon} \leq \dim G_a^b$ from the first inclusion. If we use the lemma 3.2.4, we get an inequality between accumulated multiplicities between persistence diagrams.

Lemma 3.2.7 ([4]). $\#(Dgm(f) \cap Q_{a-\epsilon}^{b+\epsilon}) \leq \#(Dgm(g) \cap Q_a^b)$ where a and b are not homological critical values. If they are homological critical values then we let a small real number $0 < \delta < \epsilon$ such that

$$\begin{aligned}
\#(Dgm(f) \cap Q_{a-\epsilon}^{b+\epsilon}) &= \#(Dgm(f) \cap Q_{a-\epsilon+\delta}^{b+\epsilon-\delta}) \\
\#(Dgm(g) \cap Q_a^b) &= \#(Dgm(g) \cap Q_{a+\delta}^{b-\delta})
\end{aligned}$$

Lemma 3.2.7 states that the total multiplicity of $Dgm(g)$ within the upper left quadrant with corner (a, b) is greater than the total multiplicity of $Dgm(f)$ inside the quadrant shrunk by ϵ . To supply analogous result for nested boxes, we need to use vector spaces that correspond to rectangular regions in the extended plane. Let $d < a < b < c$ be real numbers, all different from homological critical values of $f : X \rightarrow \mathbb{R}$. Recall that $F_a = H_i(f^{-1}(-\infty, a])$ and the dimension of it is the total multiplicity of the upper left quadrant with corner (a, a) as seen in figure 3.9.

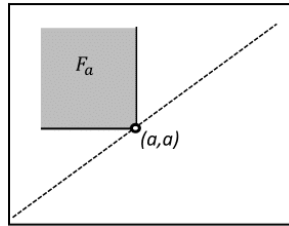


Figure 3.9: Homology group of the sublevel set $f^{-1}(-\infty, a]$

The dimension of the persistent homology group F_a^b is the total multiplicity of the upper left quadrant with corner (a, b) as seen in figure 3.10.

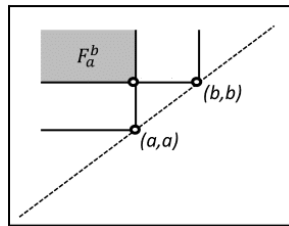


Figure 3.10: Image of F_a in F_b

A surjection $f_a^{b,c} : F_a^b \rightarrow F_a^c$ is obtained by restricting $f_b^c : F_b \rightarrow F_c$ to the vector space F_a^b .

$$\begin{array}{ccc}
 F_a & \xrightarrow{f_a^b} & F_b \\
 & \searrow f_a^c & \downarrow f_b^c \\
 & & F_c
 \end{array}$$

We have $\dim(F_a^b) = \dim(\text{Ker}(f_a^{b,c})) + \dim(\text{Im}(f_a^{b,c}))$. Let $\text{Ker}(f_a^{b,c}) = F_a^{b,c}$ then $\dim(F_a^{b,c}) = \dim(F_a^b) - \dim(F_a^c)$. This is the total multiplicity of the shaded area in figure 3.11.

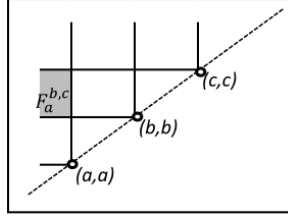


Figure 3.11: Kernel of surjection of $F_a^b \rightarrow F_a^c$.

Similarly, we have $\dim(F_{d,a}^{b,c}) = \dim(F_a^{b,c}) - \dim(F_d^{b,c})$, which is the total multiplicity of the shaded box as seen in figure 3.12.

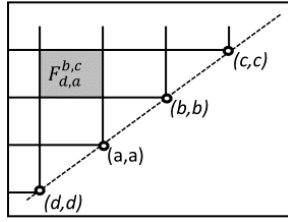


Figure 3.12: Quotient of $F_a^{b,c}$ and $F_d^{b,c}$

Lemma 3.2.8 ([4]). *Let $a < b < c < d$ be four real numbers, different from homological critical values of g and $a + \epsilon, b - \epsilon, c + \epsilon, d - \epsilon$ are not homological critical values of f . Let $M = [a, b] \times [c, d]$ be a box in $\overline{\mathbb{R}^2}$ and $M_\epsilon = [a + \epsilon, b - \epsilon] \times [c + \epsilon, d - \epsilon]$ be the shrunk box of M . Then $\#(Dgm(f) \cap M_\epsilon) \leq \#(Dgm(g) \cap M)$.*

The inequality in lemma 3.2.8 is shown by describing the total multiplicity of persistence diagram within a box as the dimension of a vector space

$$\dim F_{a+\epsilon, b-\epsilon}^{c+\epsilon, d-\epsilon} = \#(Dgm(f) \cap M_\epsilon)$$

$$\dim G_{a,b}^{c,d} = \#(Dgm(g) \cap M).$$

A consequence of the lemma 3.2.8 is that the Hausdorff distance between persistence diagrams is less than or equal to ϵ . If (m, n) is a point in $Dgm_q(f)$, then there must be a point (r, s) in $Dgm_q(g)$ at distance less than or equal to ϵ from (m, n) because the total multiplicity of $Dgm_q(g)$ inside the square $[m - \epsilon, m + \epsilon] \times [n - \epsilon, n + \epsilon]$ is at least one.

We will explain why the Hausdorff stability for persistence diagrams implies the bottleneck stability. Let us first consider the special case.

For a tame function $f : X \rightarrow \mathbb{R}$, let ξ_f be the minimum distance between two different off diagonal points or between off diagonal and the diagonal. Formally,

$$\xi_f = \min\{\|p - q\|_\infty \mid p \neq q, p \in \Delta, q \in (Dgm(f) - \Delta)\}$$

or

$$\xi_f = \min\{\|p - q\|_\infty \mid p \neq q, p, q \in (Dgm(f) - \Delta)\}.$$

Let g be another tame function $g : X \rightarrow \mathbb{R}$. The function g is called very close to f if $\|f - g\|_\infty < \xi_f/2$.

Lemma 3.2.9 completes the proof.

Lemma 3.2.9 ([4]). *Let $f, g : X \rightarrow \mathbb{R}$ be tame functions and g be very close to f . Then $d_B(Dgm(f), Dgm(g)) \leq \|f - g\|_\infty$.*

Proof. Let μ be the multiplicity of the point p in $Dgm(f) - \Delta$, that is, p is the any off diagonal point in $Dgm(f)$ and let denote \square_ϵ for the square center at p with radius $\epsilon = \|f - g\|_\infty$. Lemma 3.2.8 gives that

$$\mu \leq \#(Dgm(g) \cap \square_\epsilon) \leq \#(Dgm(f) \cap \square_{2\epsilon})$$

Since $2\epsilon < \xi_f$, p is the only point of $Dgm(f)$ in $\square_{2\epsilon}$, which gives $\#(Dgm(g) \cap \square_\epsilon) = \mu$. All points of $\#(Dgm(g) \cap \square_\epsilon)$ are mapped to p . We do this step for all off-diagonal points of $Dgm(f)$. Then the only points of $Dgm(g)$ that remain without image have distance more than ϵ from $Dgm(f) - \Delta$. Since Hausdorff distance between $Dgm(f)$ and $Dgm(g)$ is less than or equal to ϵ , these points of $Dgm(g)$ are at distance at most ϵ from the diagonal. Mapping them to their closest points on Δ yields a bijection between $Dgm(f)$ and $Dgm(g)$ where the points on Δ have infinite multiplicity. Since the bijection moves points by at most ϵ , this completes the proof. \square

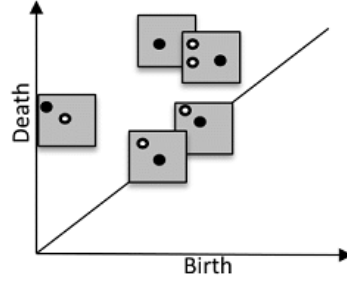


Figure 3.13: Persistence diagram of f and g

Previous section is about the stability of persistence diagrams for continuous functions. There is a combinatorial version of stability of persistence diagrams. This section is based on [7] and [6].

Let $f : X \rightarrow \mathbb{R}$ and $g : X \rightarrow \mathbb{R}$ be two monotonic functions on simplicial complex X , i.e., if σ is a face of τ then $f(\sigma) \leq f(\tau)$. Let $F : X \times [0, 1] \rightarrow \mathbb{R}$ be a straight-line homotopy defined by $F(\sigma, t) = (1 - t)f(\sigma) + tg(\sigma)$. Let denote $f_t(\sigma) = F(\sigma, t)$ and then $f_0 = f$ and $f_1 = g$. Since f and g are monotonic, f_t is monotonic for every $t \in [0, 1]$. Hence we can find compatible ordering of the simplices such that for each dimension p , we will draw persistence diagrams for f_t . For a fixed dimension p , we have a family of persistence diagrams as a multi set in $\overline{\mathbb{R}^2} \times [0, 1]$. If we draw t along a third coordinate axis, we have a three dimensional visualization of how the persistent homology changes when we go from $f_0 = f$ to $f_1 = g$. To explain this in details, let off-diagonal point of $Z_t = Dgm_p(f_t)$ be of the form $z(t) = (f_t(\sigma), f_t(\tau), t)$ where σ and τ in X . It means that when we construct simplicial complex X by adding the simplices in compatible ordering of the simplices of f_t then adding σ gives birth and adding τ gives death for p -dimensional homology class. In each interval (t_j, t_{j+1}) , the pairing (σ, τ) results in a line segment of points $z(t)$ connecting points in the planes at $t = t_j$ and $t = t_{j+1}$. If the end point of the line at $t = t_{j+1}$ lies on the diagonal, there is no line drawn after $t = t_{j+1}$. If the end point of the line at $t = t_{j+1}$ is an off-diagonal point then there is a line continuation that begins with that off diagonal point. Hence for each p , the family of persistence diagrams are connected by the lines. See figure 3.14.

Connectivity in the family of persistence diagrams says that either persistence dia-

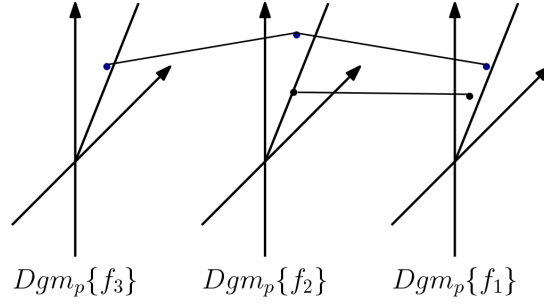


Figure 3.14: Connectivity of persistence diagrams

gram is stable or not. To clarify that let us differentiate $z(t) = (1-t)(f(\sigma), f(\tau), 0) + t(g(\sigma), g(\tau), 1)$. Then we get $(g(\sigma) - f(\sigma), g(\tau) - f(\tau), 1)$. Let us project the endpoints of the line segment of adjacent persistence diagrams into $\overline{\mathbb{R}^2}$. Then we have two points in $\overline{\mathbb{R}^2}$ with L_∞ distance equals to the $(t_{i+1} - t_i)\|f - g\|_\infty$ at the two simplices. Let v be the simplex in X that maximizes this difference, we get the L_∞ -distance between two functions $\|f - g\|_\infty = \|f - g\|$ which is an upper bound on the slope of any line segment.

Now we will explain persistence diagrams of a discrete representation of a continuous functions. Let $f, g : X \rightarrow \mathbb{R}$ be continuous functions, K be a simplicial complex, and θ be a homeomorphism from the $|K|$ to X . Let $\tilde{f}, \tilde{g} : K \rightarrow \mathbb{R}$ be the functions with $\tilde{f}(\sigma) = \max_{x \in \sigma} f(\theta(x))$ and $\tilde{g}(\sigma) = \max_{x \in \sigma} g(\theta(x)) \forall \sigma \in K$. The functions \tilde{f}, \tilde{g} are piecewise constant approximation of f and g respectively and both of them are monotone.

Theorem 3.2.10 ([6]). *For monotone functions $\tilde{f}, \tilde{g} : K \rightarrow \mathbb{R}$ and any dimension q , the bottleneck distance between the two persistence diagrams gives*

$$d_B(Dgm_q(\tilde{f}), Dgm_q(\tilde{g})) \leq \|\tilde{f} - \tilde{g}\|_\infty.$$

Proof. Consider the straight line homotopy $\tilde{f}_{t_i}(\sigma) = (1 - t_i)\tilde{f}(\sigma) + t_i\tilde{g}(\sigma)$, $0 = t_0 \leq t_1 \leq \dots \leq t_{k+1} = 1$. If σ is a face of τ then $\tilde{f}_{t_i}(\sigma) \leq \tilde{f}_{t_i}(\tau)$ because \tilde{f} and \tilde{g} are monotone. Let t_1 to t_k be the times at which the ordering of the simplices changes. Let $t_i \leq t_m < t_n < t_{i+1}$ where $0 \leq i \leq k$ and consider a pair of simplices (σ, τ) defined for the ordering that exists in the interval. Then $u_{t_m} = (\tilde{f}_{t_m}(\sigma), \tilde{f}_{t_m}(\tau))$ is a point in $Dgm_q(\tilde{f}_{t_m})$ and $u_{t_n} = (\tilde{f}_{t_n}(\sigma), \tilde{f}_{t_n}(\tau))$ is a point $Dgm_q(\tilde{f}_{t_n})$

$$\begin{aligned}
d_B(Dgm_q(\tilde{f}_{t_m}), Dgm_q(\tilde{f}_{t_n})) &\leq \|\tilde{f}_{t_m} - \tilde{f}_{t_n}\|_\infty \\
&= (t_m - t_n) \|\tilde{f} - \tilde{g}\|_\infty
\end{aligned}$$

Hence,

$$\begin{aligned}
d_B(Dgm_q(\tilde{f}), Dgm_q(\tilde{g})) &\leq \sum_{i=0}^k (d_B(Dgm_q(\tilde{f}_{t_i}), Dgm_q(\tilde{f}_{t_{i+1}}))) \\
&\leq \|\tilde{f} - \tilde{g}\|_\infty \sum_{i=0}^k (t_{i+1} - t_i).
\end{aligned}$$

□

3.3 Extended Persistence

In the persistence homology, homology classes that are born and die become paired, but essential homology classes, that is, homology classes that are born at X_i and do not die are not paired. Persistence has been extended to pair essential homology classes. In this part we work with homology with $\mathbb{Z}/2\mathbb{Z}$ coefficient and this section is based on [7], [5].

Let us recall the height function. Let $f : M \rightarrow \mathbb{R}^3$. For an immersion f of a surface and a direction \vec{u} in space, the height function, denoted by $f_{\vec{u}}$, is the projection of the immersed surface onto the directed line in the direction of \vec{u} . The value of the height function at some point m of M is found by the dot product of \vec{u} with the value of f at m . Formally, $f_{\vec{u}}(m) = \vec{u} \cdot f(m)$.

The sublevel set of the height function consists of all points with height x or less, and is denoted by $M_x = f_u^{-1}((-\infty, x])$.

To pair essential homology classes we need the notion of Reeb graph. Given a continuous map, $f : X \rightarrow \mathbb{R}$, we note that the level sets make up a partition of the

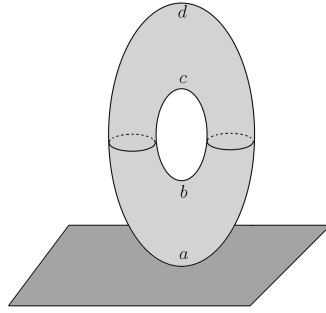


Figure 3.15: The height function of torus

topological space X . We say that $x, y \in X$ are equivalent if they belong to a common component of a level set of f . The equivalence classes of points in X are the contours of f .

Definition 3.3.1. *The Reeb Graph of f is the set of contours, denoted by $R(f)$, together with the standard quotient topology, i.e. it is defined by taking all subsets whose preimages under $\eta : X \rightarrow R(f)$ are open in X where $\eta(x)$ is the contour that contains x . Let $\phi : R(f) \rightarrow \mathbb{R}$ be the unique map whose composition with η is f , i.e., we have a commutative diagram*

$$\begin{array}{ccc}
 X & \xrightarrow{\eta} & R(f) \\
 & \searrow f & \downarrow \phi \\
 & & \mathbb{R}
 \end{array}$$

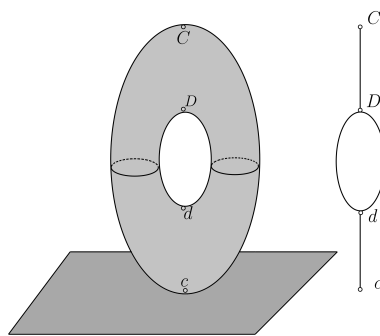


Figure 3.16: The reeb graph of torus

Let $f : M \rightarrow \mathbb{R}$ be a Morse function on a manifold of dimension $d \geq 2$. Let $c \in R(f)$ be the image of a contour in M . If $\eta^{-1}(c)$ contains a critical point then c is called the node of the Reeb graph. The nodes are connected by arcs. In figure 3.16 c, d, D and

C are nodes of the Reeb graph. Recall that the critical points have distinct function values since the function is the Morse function. This gives a bijection between the nodes of $R(f)$ and the critical points of the function.

The easiest way to pair the critical points are explained in terms of the nodes in the Reeb graph. The minimum critical point is c , the saddle points are d and D , the maximum point is C in figure 3.16. We pair the lowest node with the highest node. Each saddle corresponds to node which either forks up or down. A loop in the Reeb graph has the minimum at its lowest upfork and the maximum at its highest downfork, and the two forks span the loop. Each up-fork is to be paired with the lowest down-fork. In figure 3.16 d is paired with D and c is paired with C .

Now, we will explain how to extend the sequence of homology groups induced by the inclusions. Let M be a d -dimensional manifold and $f : M \rightarrow \mathbb{R}$ be a Morse function on M with critical values $a_1 < a_2 < \dots < a_n$. We choose interleaved values b_i , with the following order $b_0 < a_1 < b_1 < a_2 < \dots < a_n < b_n$. Let us recall that the sublevel set is $M_{b_i} = f^{-1}(-\infty, b_i]$ and the superlevel set is $M^{b_i} = f^{-1}[b_i, \infty)$. Since $M_{b_0} \subseteq M_{b_1} \subseteq \dots \subseteq M_{b_n}$ we have the following sequence of homology groups induced by the inclusions.

$$0 = H_p(M_{b_0}) \rightarrow H_p(M_{b_1}) \rightarrow \dots \rightarrow H_p(M_{b_n}).$$

We extend this sequence by applying Poincaré duality to $H_p(M_{b_n})$. Let us recall that for a compact d -manifold without boundary, Poincaré duality gives an isomorphism $H_p(M; \mathbb{Z}_2) \cong H^{d-p}(M; \mathbb{Z}_2)$. Note that the inclusion $M_{b_{m-1}} \subseteq M_{b_m}$ induces map $H^{d-p}(M_{b_m}) \rightarrow H^{d-p}(M_{b_{m-1}})$.

$$0 = H_p(M_{b_0}) \rightarrow \dots \rightarrow H_p(M_{b_n}) \cong H^{d-p}(M_{b_n}) \rightarrow \dots \rightarrow H^{d-p}(M_{b_0}) = 0$$

Lefschetz duality yields $H_p(M, \partial M; \mathbb{Z}_2) \cong H^{d-p}(M; \mathbb{Z}_2)$ where M is compact, d -manifold with compact boundary ∂M . If we apply Lefschetz duality to each cohomology groups in the sequence we will get

$$H_p(M_{b_n}) \cong H_p(M_{b_n}, \partial M_{b_n}) \rightarrow H_p(M_{b_{n-1}}, \partial M_{b_{n-1}}) \rightarrow \dots \rightarrow H_p(M_{b_0}, \partial M_{b_0}).$$

We can replace the boundaries of the sublevel sets by those of the corresponding superlevel sets in the above sequence, since

$$\partial M_{b_i} = \partial M^{b_i} = f^{-1}(b_i)$$

and we have the following sequence

$$H_p(M_{b_n}, \partial M^{b_n}) \rightarrow H_p(M_{b_{n-1}}, \partial M^{b_{n-1}}) \rightarrow \dots \rightarrow H_p(M_{b_0}, \partial M^{b_0}).$$

Let us recall Excision Theorem since we apply it to each homology group

Theorem 3.3.2. [12] *Given subspaces $Z \subset A \subset X$ such that the closure of Z is contained in the interior of A , then the inclusion $(X - Z, A - Z) \hookrightarrow (X, A)$ induces isomorphism $H_p(X \setminus Z, A \setminus Z) \rightarrow H_p(X, A)$ for all p . Equivalently, for subspaces $A, B \subset X$ whose interiors cover X , the inclusion $(B, A \cap B) \hookrightarrow (X, A)$ induces isomorphism $H_p(B, A \cap B) \rightarrow H_p(X, A)$ for all p .*

We end up with the following sequence which is the *extended persistence sequence*

$$0 = H_p(M_{b_0}) \rightarrow \dots \rightarrow H_p(M_{b_n}) \rightarrow H_p(M, M^{b_n}) \rightarrow \dots \rightarrow H_p(M, M^{b_0}) = 0.$$

Given such an extended persistence sequence, we get homomorphisms $f_p^{i,j} : X_i \rightarrow X_j$ for every $0 \leq i \leq j \leq 2n$ where

$$X_i = \begin{cases} H_p(M_{b_i}), & \text{if } i \leq n \\ H_p(M, M^{b_{2n-i}}), & \text{if } i \geq n + 1 \end{cases} \quad (3.2)$$

Definition 3.3.3. *The p -th extended persistent homology groups is $H_p^{i,j} = \text{Im}(f_p^{i,j})$. Its rank is the p -th extended persistent Betti numbers denoted as $\beta_p^{i,j}$.*

Theorem 3.3.4 ([5], Duality Theorem). *Let f be a real valued function on d -manifold M . By Lefschetz duality we have*

$$\text{Ord}_r(f) = \text{Rel}_{d-r}^T(f)$$

$$\text{Rel}_r(f) = \text{Ord}_{d-r}^T(f)$$

$$\text{Ext}_r(f) = \text{Ext}_{d-r}^T(f).$$

The superscript T denotes the reflection along the main diagonal of the persistence diagram. The second version of this theorem states that a real valued function f on a d -manifold has persistence diagrams satisfying, $Dgm_r(f) = Dgm_{d-r}^T(f) \forall r$.

Theorem 3.3.5 ([5], Symmetry Theorem). *Let f be a real valued function on d -dimensional manifold then*

$$Ord_r(f) = Ord_{d-r-1}^R(-f)$$

$$Ext_r(f) = Ext_{d-r}^R(-f)$$

$$Rel_r(f) = Rel_{d-r-1}^R(-f).$$

The superscript R denotes the reflection along the minor diagonal, mapping (x, y) to $(-y, -x)$.

We extended persistence of manifolds by using Poincaré and Lefschetz duality. In this section we explain extended persistence sequence of simplicial complex. To do that we need some basic notions such as lower star, lower link of vertex, and vertex ordering filtration.

Let us recall that the star of a vertex v of a simplicial complex K is the set of cofaces of v in K and the link consists of all faces of simplices in the star that do not belong to the star:

$$Stv = \{\tau \in K | v \in \tau\}$$

$$Lkv = \{\sigma \in K - Stv | \sigma \subseteq \tau \in Stv\}.$$

The *lower star* of a vertex v consists of all simplices in the star for which v is the vertex with maximum function value,

$$St_{-}v = \{\tau \in Stv | x \in \tau \Rightarrow f(x) \leq f(v)\}.$$

The *lower link* consists of all simplices in the link whose vertices have smaller function value than v ,

$$Lk_{-}v = \{\tau \in Lkv | x \in \tau \Rightarrow f(x) < f(v)\}.$$

Let f be an injective, real valued function on vertices of simplicial complex K , with order $f(v_1) < f(v_2) < \dots < f(v_n)$. Let K_j be the subcomplex of K spanned by the first j vertices, $K_j = \{\tau \in K \mid \langle v_1, v_2, \dots, v_j \rangle\}$. If we add lower star of v_j to K_{j-1} then we get K_j . Such filtration is called ascending vertex ordering filtration,

$$\emptyset = K_0 \subset K_1 \subset \dots \subset K_n = K.$$

In the same way, let L_{n-j} be the subcomplex of K spanned by the last $n - j$ vertices. More formally, $L_{n-j} = \{\tau \in K \mid \langle v_{n-j+1}, v_{n-j+2}, \dots, v_n \rangle\}$. If we add upper star of v_{j+1} to L_{n-j-1} then we get L_{n-j} . Such filtration is called descending vertex ordering filtration

$$\emptyset = L_0 \subset L_1 \subset \dots \subset L_n = K.$$

Ascending vertex ordering filtration induces a sequence of homology groups,

$$0 = H_m(K_0) \rightarrow \dots \rightarrow H_m(K_n).$$

We extend this sequence by using Poincaré duality isomorphism,

$$0 = H_m(K_0) \rightarrow \dots \rightarrow H_m(K_n) \rightarrow H^{d-m}(K_n) \rightarrow \dots \rightarrow H^{d-m}(K_0) = 0.$$

Using the excision and Lefschetz duality, we finally get

$$0 = H_m(K_0) \rightarrow \dots \rightarrow H_m(K_n) \rightarrow H_m(K, L_0) \rightarrow \dots \rightarrow H_m(K, L_n) = 0.$$

We write $K_{n+i} = (K, L_i)$, $K_n = (K, \emptyset)$ for $0 \leq i \leq n$ and $H_l^j = H_l(K_j)$, for $0 \leq j \leq 2n$. The extended sequence of homology groups is

$$0 = H_m^0 \rightarrow \dots \rightarrow H_m^n \rightarrow \dots \rightarrow H_m^{2n} = 0.$$

A class that is born at K_i or $(K, L_i) = K_{n+i}$ and dies entering K_j or $(K, L_j) = K_{n+j}$ has index extended persistence $|j - i|$.

We will analyse what happens when one goes from a homology group to the next one in the extended sequence. Firstly, we start with an ascending filtration and consider the kernels and cokernels of the map $h_p^{i,m} : H_p(K_i) \rightarrow H_p(K_m) = H_p(K)$. For fixed p and i , let

$$\begin{aligned} K_p^i &= \text{Ker}(h_p^{i,m}) \\ C_p^i &= H_p(K)/\text{Im}h_p^{i,m} \\ \kappa &= K_{p-1}^{i-1} \rightarrow K_{p-1}^i \\ c &= C_p^{i-1} \rightarrow C_p^i \end{aligned}$$

where C_p^i is the cokernel and κ, c are the maps induced by the inclusions $K_{i-1} \subseteq K_i \subseteq K$.

Note that K_p^i consists of all inessential homology classes in $H_p(K_i)$, the ones that die before reaching K . The cokernel consists of all new essential homology classes in $H_p(K)$, the ones that have no pre-image in $H_p(K_i)$.

If $\text{ker } \kappa \neq 0$ then there is a non-trivial class in H_{p-1}^{i-1} that goes to zero in H_{p-1}^i . It means that the class dies and the dimension $(p-1)$ homology group decreases in rank by one, and we have a negative p -simplex that paired with an earlier, positive $(p-1)$ -simplex. If $\text{coker } \kappa \neq 0$ then there is a new class in H_{p-1}^i that is inessential in K . It means that the class is born at K_i , the dimension $(p-1)$ homology group increases in rank by one, and we have a positive $(p-1)$ -simplex that will get paired with a negative p -simplex later. If $\text{ker } c \neq 0$ then there is a new class in H_p^i that is essential in K . This class is born at K_i , the dimension p homology group increases in rank by one, and we have a positive p -simplex that will not get paired.

To relate the homology changes of L_i to that of (K, L_i) we use long exact sequence for the pair (K, L_i) ,

$$\dots \rightarrow H_p(L_i) \rightarrow H_p(K) \rightarrow H_p(K, L_i) \rightarrow H_{p-1}(L_i) \rightarrow \dots$$

Let write K_p^i for the kernel of $H_p(L_i) \rightarrow H_p(K)$ and C_p^i for the cokernel of $H_p(L_i) \rightarrow H_p(K)$.

$$\begin{array}{ccccccc}
\longrightarrow & H_p(L_{i-1}) & \longrightarrow & H_p(K) & \longrightarrow & H_p(K, L_{i-1}) & \longrightarrow & H_{p-1}(L_{i-1}) \\
& \downarrow & & \downarrow & & \downarrow & & \downarrow \\
\longrightarrow & H_p(L_i) & \longrightarrow & H_p(K) & \longrightarrow & H_p(K, L_i) & \longrightarrow & H_{p-1}(L_i)
\end{array}$$

We then get the short exact sequence $0 \rightarrow C_p^i \rightarrow H_p(K, L_i) \rightarrow K_{p-1}^i \rightarrow 0$. Since we work with $\mathbb{Z}/2\mathbb{Z}$ coefficient this sequence splits, then $H_p(K, L_i) \cong C_p^i + K_{p-1}^i$. We have the following commutative diagram:

$$\begin{array}{ccccccc}
0 & \longrightarrow & C_p^{i-1} & \longrightarrow & H_p(K, L_{i-1}) & \longrightarrow & K_{p-1}^{i-1} & \longrightarrow & 0 \\
& & \downarrow c & & \downarrow & & \downarrow \kappa & & \\
0 & \longrightarrow & C_p^i & \longrightarrow & H_p(K, L_i) & \longrightarrow & K_{p-1}^i & \longrightarrow & 0
\end{array}$$

When we go from (K, L_{i-1}) to (K, L_i) , we get L_i by adding λ_i to L_{i-1} .

In a descending filtration, three cases have been considered:

If $\ker \kappa \neq 0$ λ_i is a negative p -simplex and the dimension $(p-1)$ homology group decreases in rank by one. For the dimension p relative homology group we have $\text{rank} H_p(K, L_i) = \text{rank} H_p(K, L_{i-1}) - 1$.

If $\text{coker} \kappa \neq 0$ λ_i is a positive $(p-1)$ -simplex and the dimension $(p-1)$ homology group increases in rank by one. For the dimension p relative homology group we have $\text{rank} H_p(K, L_i) = \text{rank} H_p(K, L_{i-1}) + 1$.

If $\ker c \neq 0$ λ_i is a positive p -simplex and the dimension p homology group increases in rank by one. $\text{rank} H_p(K, L_i) = \text{rank} H_p(K, L_{i-1}) - 1$.

All of them are summarised in three rules:

A dimension p homology class of M^b dies at the same time a dimension $(p+1)$ relative homology class of (M, M^b) dies.

An inessential dimension p homology class of M^b gets born at the same time a dimension $(p+1)$ relative homology class of (M, M^b) gets born.

An essential dimension p homology class of M^b gets born at the same time a dimen-

sion p relative homology class of (M, M^b) dies.

Example 3.3.6. Consider 2-manifold torus in figure 3.17. Morse function will be the height function. In this figure there are 4 critical points c_1, c_2, c_3, c_4 . We choose interleaved values b_1, b_2, b_3, b_4 .

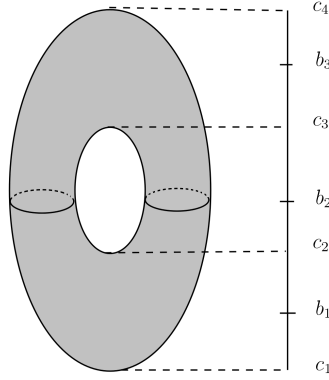


Figure 3.17: 2-manifold torus

We track how the homology groups are changing from the sublevel set M_{j-1} to M_j for $j = 1, \dots, 4$.

M_{b_1} : is homeomorphic to a disc.

M_{b_2} : is homeomorphic to a tube, i.e., 0-dimensional class lives and a 1-dimensional class is born.

M_{b_3} : is homeomorphic to a torus missing one point, i.e., another 1-dimensional class is born.

M_{b_4} : is the 2-dimensional homology class. In this example all homology classes are essential, because all classes are born, but they do not die. So we represent them by a single dot at infinity in the persistence diagrams of dimension 0, 1 and 2 as seen in figure 3.18. When we go up c_1 gives the birth of classes in H_0 , c_2, c_3 give the birth of classes in H_1 and c_4 give the birth of classes in H_2 .

To pair these essential homology classes we need extended persistence homology. We look at relative homology groups, starting with $H_p(M, M^{b_4})$ which is $H_p(M)$.

$$H_p(M) = \begin{cases} \mathbb{Z}_2 + \mathbb{Z}_2, & \text{if } p = 1 \\ \mathbb{Z}_2, & \text{if } p = 0, p = 2 \end{cases} \quad (3.3)$$

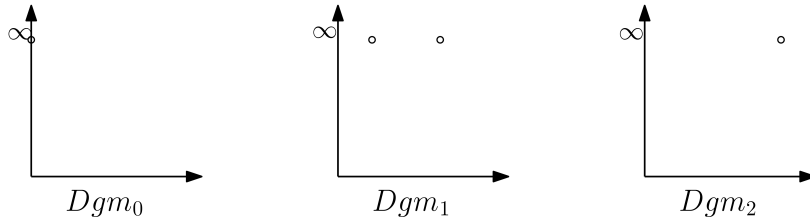


Figure 3.18: Ordinary persistence diagrams of dimension 0,1, and 2 from left to right

By rule 3, an essential dimension 0 homology class of M^{b_3} gets born at the same time a dimension 0 relative homology class of (M, M^{b_3}) dies. So coming down c_4 kills the class in H_0 . Furthermore c_3, c_2 kill the classes in H_1 and c_1 kills the class in H_2 . As explained in the Reeb graph (c_1, c_4) is the pair in dimension 0. In dimension 1, (c_2, c_3) and (c_3, c_2) are the pairs. In dimension 2, (c_4, c_1) is the pair as seen in below figure.

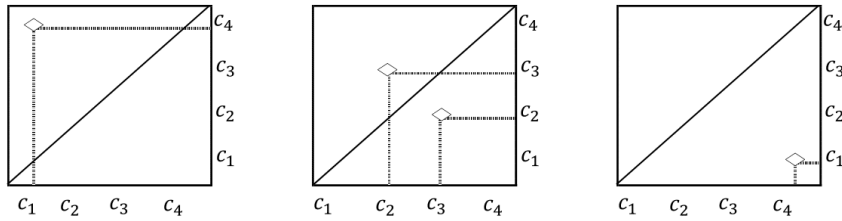


Figure 3.19: Extended persistence diagrams of dimension 0,1 and 2 from left to right

CHAPTER 4

THE PURPOSE OF THE STUDY AND METHOD

Let M be an n -dimensional simplicial complex and suppose that for $0 = t_0 < \dots < t_m = 1$, we have a discrete Morse function $f_{t_i} : M \rightarrow \mathbb{R}$. We call the simplicial complex $M_i = M \times t_i \subset M \times I$ as slice. In our method, there are two cases to consider. In the first one, the triangulations in each slice are the same and in the second one the triangulations are different on each slice. Recall that discrete bifurcation diagrams show whether or not the critical cells in each slice live in the adjacent slices or new critical cells appear in the next slice. In this part we give a method for drawing discrete bifurcation diagrams by using persistence homology.

In the first case, we find the sublevel set for each slice to construct filtration. When a negative simplex is paired with a youngest positive simplex, they become persistence pair and are represented as a point on the persistence diagram. For each dimension, the bottleneck distances are computed. We draw a box of side length twice the bottleneck distance centered at the point which corresponds to the critical cell in the persistence diagram. We overlay the persistence diagrams. If the points on the persistence diagrams lie in the box, then we draw lines between corresponding cells which gives a discrete bifurcation diagram for each dimension less than n .

When the triangulations on each slice are different, King et. al. [14] consider the common subdivision of both slices and state an algorithm to find the refinement of discrete vector fields. Refinement enables us to construct the same triangulations for each slice so that we apply the solution method of the first case. It is seen that when the node is added on the critical edge, the cell is divided. Hence the bottleneck distance of dimension 1 decreases. It is observed that the bottleneck distance of dimension 0 is not changed during the process of refinement. In the application, if

we need to track the critical cells of dimension 0, we don't need to make refinement when we use persistence homology. Since before refinement and after the refinement the bottleneck distance of dimension 0 is the same.

Note that we can not draw persistence diagram for dimension n except for n -dimensional essential homology class, because persistence pair of the n -dimensional homology class is an $n + 1$ -dimensional simplex. To find the persistence pair of the essential homology class and n -dimensional class, a sequence of homomorphism is extended [5]. With the application of the theorem 3.3.4, a persistence diagram for dimension n is drawn and the method stated in the second paragraph is implemented. Note that theorem 3.3.4 is applicable for the compact manifold with boundary, so that Lefschetz duality holds.

In addition, the stability of persistence diagrams is covered in section 3.2. In the first part of the section the stability of persistence diagrams for continuous functions is explained. A combinatorial version of stability of persistence diagrams is given in the last part of the section. We use it in our study.

As an application, leukemic cells of leukemic mouse are used as data set. There is set of images of leukemic cells taken in 10 days. Each image is in png format and is loaded in Matlab. So that we obtain the resolution of the $2D$ grayscale. The sequence of images are modelled with a vertex for each pixel and each adjacent vertex is connected by edge. With algorithm in [15], the extended discrete gradient vector fields are found. The birth and death algorithm in [14] gives in discrete bifurcation diagram of the vertices. We track the minimal vertices by using persistence diagrams of images. To do that, filtrations of images have been found and then persistence diagrams of them are compared as stated in the second paragraph.

In the following part, we explain how to draw discrete bifurcation diagram step by step by starting with a simple simplicial complex of circle. The algorithm is also applied for the 2-dimensional simplicial complex, such as torus. Then the algorithm is generalised for the higher dimensional simplicial complex. At the end we state the outline of the algorithm.

4.1 Method for the First Case

Let $F : X \times \{t_i\} \rightarrow \mathbb{R}$ and $G : X \times \{t_{i+1}\} \rightarrow \mathbb{R}$ be discrete Morse functions on circle, X . In this case the triangulations on each circle is the same as in figure 4.1. Critical cells of 0- and 1- dimension are coloured with red circles and red lines respectively.

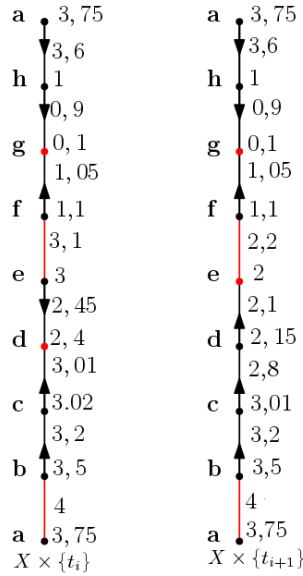


Figure 4.1: Discrete Morse functions F and G on circle from left to right

We will use persistence diagrams to find which critical cells on $X \times \{t_i\}$ go to the critical cells on $X \times \{t_{i+1}\}$ in the discrete bifurcation diagram. Firstly, the filtration for each slice will be obtained by using the sublevel sets.

Let $0.1 \leq 0.9 \leq 1 \leq 1.05 \leq 1.1 \leq 2.4 \leq 2.45 \leq 3 \leq 3.01 \leq 3.02 \leq 3.1 \leq 3.2 \leq 3.5 \leq 3.6 \leq 3.75 \leq 4$ be the function values of the simplices in $X \times \{t_i\}$. Recall that $X_i = f^{-1}(-\infty, a_i]$, is a subcomplex of X for every $a_i \in \mathbb{R}$. Hence

$X_0 = f^{-1}(-\infty, 0.1]$ is the positive simplex g .

$X_1 = f^{-1}(-\infty, 0.9]$ is the edge denoted by $[g, h]$.

$X_2 = f^{-1}(-\infty, 1]$ is the same as X_1 . Since the negative simplex $[g, h]$ bounds the youngest vertex h , they become persistence pair. Note that the vertex h and the edge $[g, h]$ enter the filtration at the same time and hence they are represented as a point on the diagonal of the persistence diagram. See figure 4.2.

$X_3 = f^{-1}(-\infty, 1.05]$ is the union of X_2 and the edge $[f, g]$.

$X_4 = f^{-1}(-\infty, 1.1]$ is the same as X_3 . Note that adding the vertex f and the edge $[f, g]$ makes them persistence pair.

$X_5 = f^{-1}(-\infty, 2.4]$ is the union of X_4 and the positive simplex d .

$X_6 = f^{-1}(-\infty, 2.45]$ is the union of X_5 and the edge $[d, e]$. $X_6 = X_7$. In this level, $[d, e]$ and the youngest vertex e get paired.

$X_8 = f^{-1}(-\infty, 3.01]$ is the adding of the negative simplex $[c, d]$ to X_7 . The positive simplex c is paired with $[c, d]$.

Similarly, $X_9 = X_8$.

$X_{10} = f^{-1}(-\infty, 3.1]$. The positive simplex d is paired with $[e, f]$.

$X_{11} = X_{12}$. In this level $[b, c]$ and b become persistence pair.

The last persistence pair is the vertex a and the edge $[a, h]$. Finally, adding the edge $[a, b]$ completes the filtration.

The outline of finding the persistence pair in this solution is:

Algorithm 1 persistence pair

- 1: **for** $i = 1, \dots, n$ **do**
 - 2: **if** $X_{i+1} \setminus X_i = \sigma_{i+1}$ is a negative simplex **then**
 - 3: pair the youngest positive simplex with σ_{i+1}
 - 4: **else**
 - 5: a positive simplex with no persistence pair becomes an essential homology class
 - 6: **end if**
 - 7: **end for**
-

In the same way we construct the filtration for the next slice.

Let $0.1 \leq 0.9 \leq 1 \leq 1.05 \leq 1.1 \leq 2 \leq 2.1 \leq 2.15 \leq 2.2 \leq 2.8 \leq 3.01 \leq 3.2 \leq 3.5 \leq 3.6 \leq 3.75 \leq 4$ be the function values of the simplices in $X \times \{t_{i+1}\}$.

$X_0 = f^{-1}(-\infty, 0.1]$ is the vertex g and is a positive simplex.

$X_1 = f^{-1}(-\infty, 0.9]$ is the edge denoted by $[g, h]$.

$X_2 = f^{-1}(-\infty, 1]$ is the same as X_1 . The edge $[g, h]$ and the vertex h , become persistence pair.

$X_3 = f^{-1}(-\infty, 1.05]$ is the union of X_2 and the edge $[f, g]$.

$X_4 = f^{-1}(-\infty, 1.1]$ is the same as X_3 . In the same way, adding the vertex f and the edge $[f, g]$ makes them persistence pair.

$X_5 = f^{-1}(-\infty, 2]$ is the union of X_4 and the positive simplex e .

$X_6 = f^{-1}(-\infty, 2.1]$ is the union of X_5 and the edge $[d, e]$. $X_6 = X_7$. In this level, $[d, e]$ and the youngest vertex d become persistence pair.

$X_8 = f^{-1}(-\infty, 2.2]$ is the adding of the edge $[e, f]$ to X_7 . The negative simplex $[e, f]$ is paired with e which is born in X_5 . Remark that they are critical cells.

$X_9 = f^{-1}(-\infty, 2.8]$ is the adding of the negative simplex $[c, d]$ to X_8 .

Similarly, $X_{10} = X_9$. Hence $[c, d]$ and c become persistence pair.

$X_{11} = X_{12}$. In this level $[b, c]$ and b become persistence pair.

The last persistence pair for this slice is the vertex a and the edge $[a, h]$. Finally, adding the edge $[a, b]$ completes the filtration and creates a cycle.

So for an ordered function values on each slice, there is a sequence $X_0 \subseteq X_2 \dots \subseteq X_{15}$. Lemma 3.1.3 says that the inclusion induces a sequence of homomorphism. The homological changes of sublevel sets are followed via this sequence.

Let $Dgm_q(F)$ and $Dgm_q(G)$ be persistence diagrams of F and G respectively for each dimension $q = 0, 1$. In figure 4.2, the essential homology classes of dimension 0 are g for both of the slices and are denoted at infinity on the persistence diagrams.

The essential homology classes of dimension 1 are $[a, b]$ for both of the slices and are denoted at infinity on the persistence diagrams. See figure 4.3.

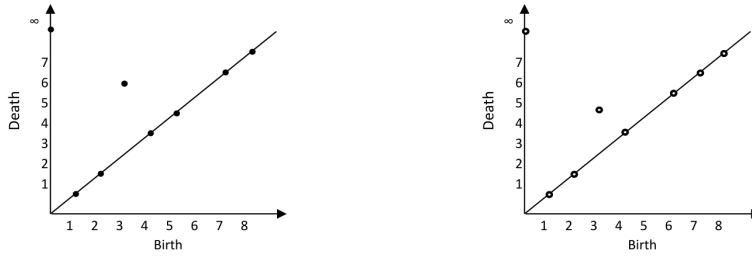


Figure 4.2: Persistence diagrams of 0-dimension

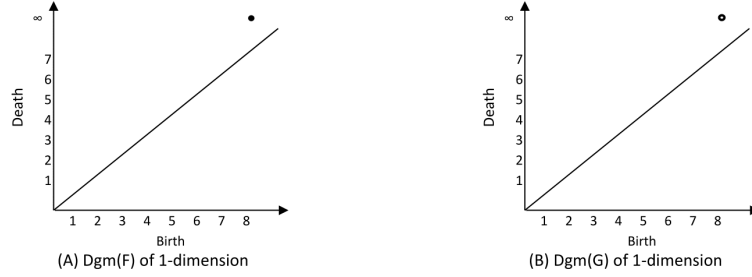


Figure 4.3: Persistence diagrams of 1-dimension

The bottleneck distance between $Dgm(F)$ and $Dgm(G)$ is:

$$d_B(Dgm(F), Dgm(G)) = \inf_{\rho: X \rightarrow Y} \sup_{x \in X} \|x - \rho(x)\|,$$

where ρ ranges over all bijections from $Dgm(F)$ to $Dgm(G)$ and $x \in Dgm(F)$, $\rho(x) \in Dgm(G)$. We compute the bottleneck distance as 1 for 0-dimension.

Now, we draw a square of side length twice the bottleneck distance centered at the black point of $Dgm(F)$ and then overlay the two persistence diagrams. The white point of $Dgm(G)$ lies in this box as in figure 4.4.

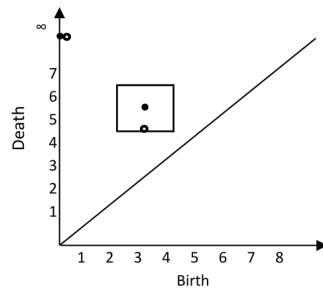


Figure 4.4: Overlaid persistence diagrams of 0-dimension

In figure 4.4, the critical cell e of G corresponds to white circle and the critical cell d of F corresponds to the black circle and they lie in the box. Therefore we join them

to draw the discrete bifurcation diagram of dimension 0.

We consider the extended persistence homology to say more things about essential homology classes for each slices.

Let a_1, a_2, a_3, a_4 be the function values of $g, d, [e, f]$ and $[a, b]$ respectively on $X \times \{t_i\}$. Then $a_1 < a_2 < a_3 < a_4$ is an ordered homological critical values of the first slice. Recall that for an interleaved values $b_0 < a_1 < b_1 < a_2 < b_2 < a_3 < b_3 < a_4 < b_4$ the sublevel set is $M_{b_i} = F^{-1}(-\infty, b_i]$. The inclusion in the sublevel set induces a homomorphism sequence.

Let a'_1, a'_2, a'_3, a'_4 be the function values of $g, e, [e, f]$ and $[a, b]$ respectively on $X \times \{t_{i+1}\}$.

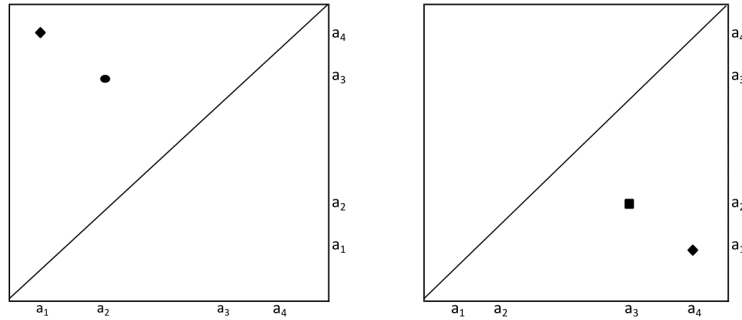


Figure 4.5: Ordinary, extended and relative persistence diagrams of F

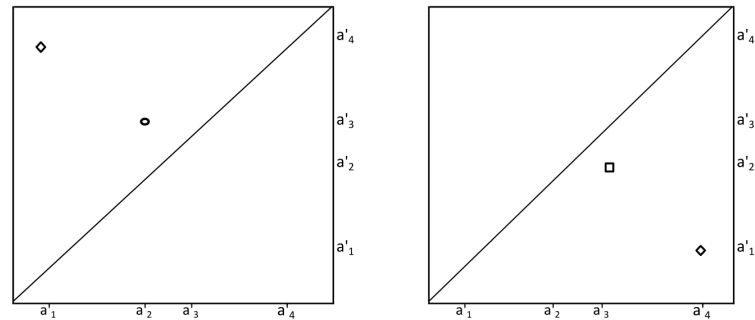


Figure 4.6: Ordinary, extended and relative persistence diagrams of G

In the ordinary sequence of homomorphism, we have seen that d is paired with $[e, f]$. The left unpaired cells are the essential homology classes g and $[a, b]$ which are global minimum and global maximum cell. Hence they are paired by [5] and is denoted as diamond in figure 4.5.

The ordinary, extended and relative persistence diagrams are defined by circle, diamond and square as in figure 4.5, 4.6 and 4.7.

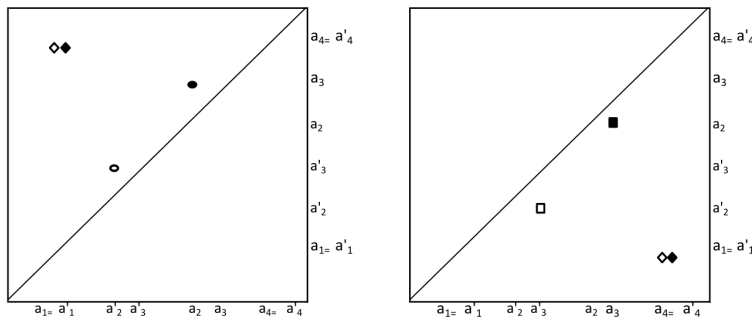


Figure 4.7: Overlaid persistence diagrams of F and G

Persistence duality gives that $Ord_0(F) = Rel_1^T(F)$ as seen in figure 4.5 and $Ord_0(G) = Rel_1^T(G)$ as seen in figure 4.6. We overlay the two figures as in figure 4.7. This enables us to say that 1-dimensional critical cell $[e, f]$ of G is connected to 1-dimensional critical cell $[e, f]$ of F in the discrete bifurcation diagram.

In this part, we will draw discrete bifurcation diagram for the discrete Morse functions with the help of persistence diagrams. We also draw discrete bifurcation diagrams by using the birth and death algorithm to compare both of the discrete bifurcation diagrams.

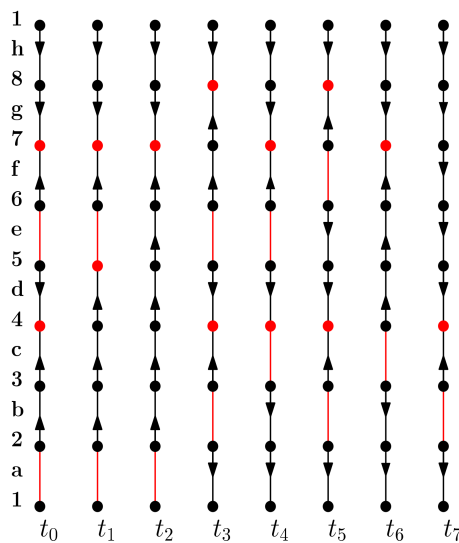


Figure 4.8: A family of discrete gradient fields on circle

Let M be a circle and suppose that for $0 = t_0 < \dots < t_7 = 1$, there is a discrete Morse function $f_{t_i} : M \rightarrow \mathbb{R}$. The vertices are labelled from 1 to 8 and the edges are labelled from a to h as in figure 4.8. For each slices, the filtrations are found and then persistence diagrams are drawn and the bottleneck distances for each dimension are computed. The stability of persistence diagrams are checked and found that they are stable. Circle has one 0- and one 1-dimensional essential homology classes. So the persistence pairs of essential homology classes are found by using extended persistence. The resulted discrete bifurcation diagrams are seen in figure 4.10.

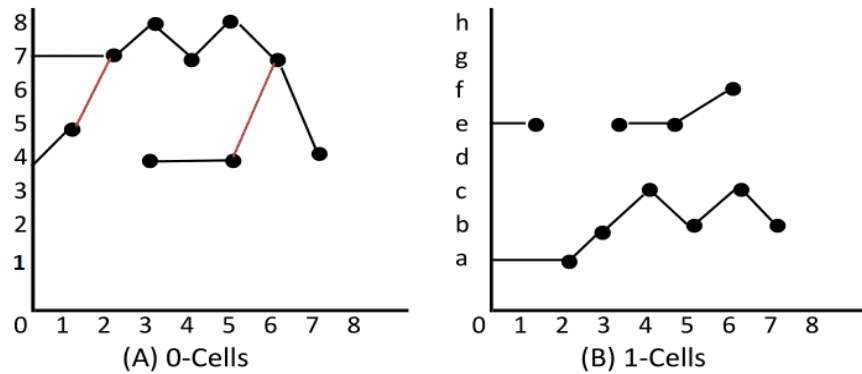


Figure 4.9: Connectivity diagrams associated with the example in figure 4.9

We want to compare our result with the birth and death algorithm. We firstly, consider the forward case and then backward case. In the figure 4.9, the black lines show the strong connections between critical cells. The red lines show the connections of the critical cells in one direction in adjacent slices.

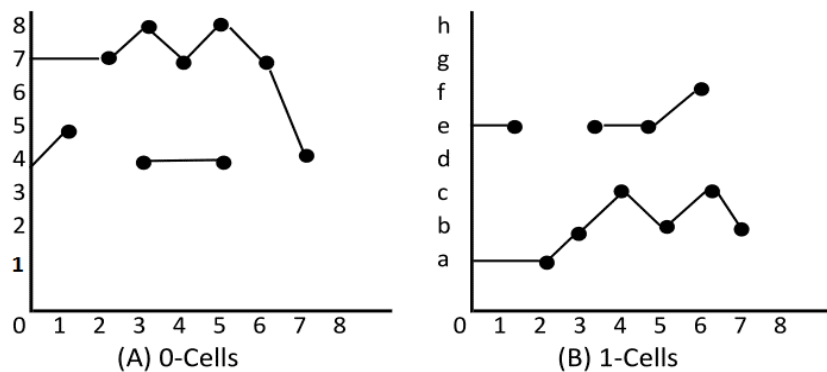


Figure 4.10: Strong connectivity diagrams associated with the example in figure 4.9

When the persistence diagrams are stable, the discrete bifurcation diagram obtained by the birth and death algorithm is the same as the figure 4.10. If the persistence

diagrams are not stable the result is different. To make it concrete, let us take slice $M \times t_6$ and change the place of 0-dimensional critical cell from 7 to 4. Let us denote this slice as $M \times t'_6$. On the new slice 4 is the 0- and c is the 1-dimensional essential homology classes. Let us take another slice $M \times t_5$ from figure 4.8 without any changes as seen in figure 4.11.

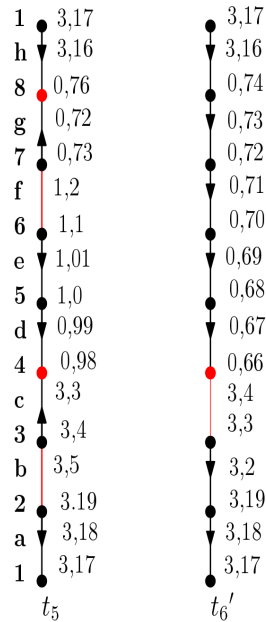


Figure 4.11: Discrete Morse function on circle

On $M \times t_5$, 8 and b are the essential homology classes, and 4 has a persistence pair f . The bottleneck distances are 1.5 for dimension 0 and 1 for dimension 1. The bottleneck distance for dimension 0 is greater than L_∞ norm of difference of functions, i.e., persistence diagram of 0-dimension is not stable. In our algorithm, the essential homology class 4, on $M \times t'_6$ must go to the essential homology class 8 on $M \times t_5$, because both of them are denoted at infinity on the persistence diagrams. But in the birth and death algorithm, there is a strong connection between critical cell 4 on $M \times t_5$ and 4 on $M \times t'_6$.

Now we want to consider what will happen if the critical cells are born at the same time on one slice. Let $F : M \times \{t_i\} \rightarrow \mathbb{R}$ and $G : M \times \{t_{i+1}\} \rightarrow \mathbb{R}$ be discrete Morse functions on circle as in figure 4.12. Let two 0-dimensional critical cells with the same values be on $M \times \{t_i\}$. We draw persistence diagrams of $M \times \{t_i\}$ and $M \times \{t_{i+1}\}$. We find that the bottleneck distance of persistence diagrams for dimension 0 and 1

are equal to 1. In the computation, one of the critical cell on $M \times \{t_i\}$ is paired with the critical cell $[c, d]$ at X_2 . Therefore essential homology class for dimension 0 is not identified. This does not contradict anything, because finding the persistence pair requires different critical values.

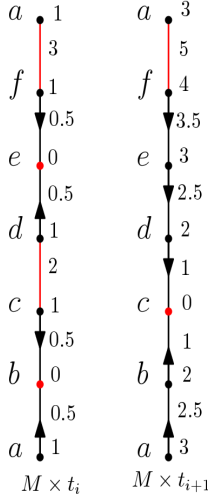


Figure 4.12: Discrete gradient fields

In this part, we want to draw discrete bifurcation diagram for the higher dimensional topological space by using persistence diagrams and compare the results with the birth and death algorithm.

Let $f : X \times \{t_i\} \rightarrow \mathbb{R}$ and $g : X \times \{t_{i+1}\} \rightarrow \mathbb{R}$ be the discrete Morse functions on torus, X . Each vertices and edges have function values. Only the function values of vertices are seen in the below figures. Remark that, the triangulation on each torus is the same as in figure 4.13. Red points are the 0-, red lines are the 1-, green triangles are the 2- dimensional critical cells of torus.

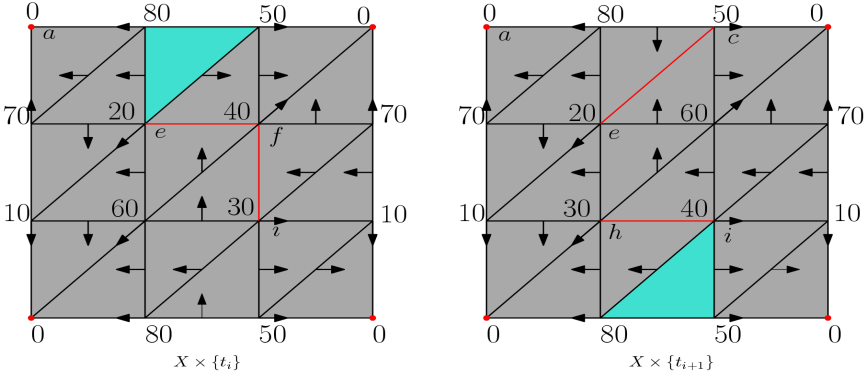


Figure 4.13: Discrete Morse function on torus

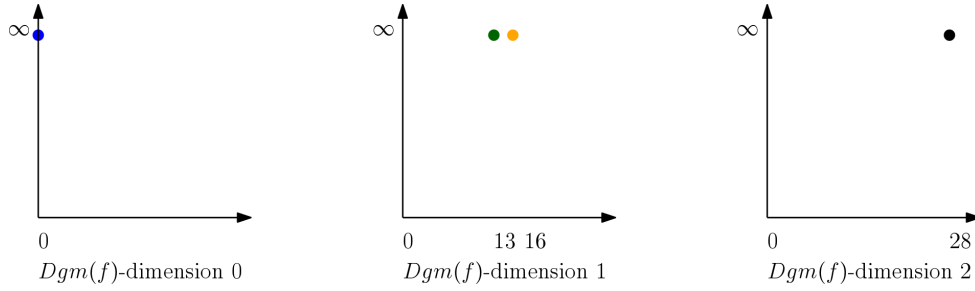


Figure 4.14: Persistence diagrams of $X \times \{t_i\}$

Each torus has one 0-, two 1- and one 2-dimensional essential classes. In figure 4.14, the birth and death of the $[f, i]$ and $[e, f]$ on $X \times \{t_i\}$ are denoted by green and yellow circles respectively. Similarly, the birth and death of $[h, i]$ and $[c, e]$ on $X \times \{t_{i+1}\}$ are denoted by green and yellow squares in figure 4.15. The bottleneck distances are 0 for dimension 0 and 3 for dimension 1. Remark that red point is the minimum, red lines are the saddle and green triangles are the maximum critical cells.

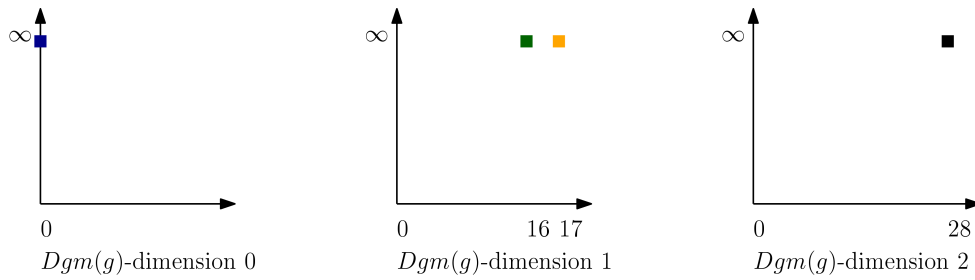


Figure 4.15: Persistence diagrams of $X \times \{t_{i+1}\}$

Since there are two 1-dimensional critical cells, we have to show which critical cells have strong connections in the discrete bifurcation diagram. We draw the squares of side length twice the bottleneck distance centered at the points of the persistence diagram of $X \times \{t_i\}$. Then two persistence diagrams are superimposed. It is seen that yellow square lies in the box centered with yellow circle. This implies that we can connect $[e, f]$ and $[c, e]$ in the discrete bifurcation diagram. Similarly, birth and death algorithm brings about strong connection between $[e, f]$ and $[c, e]$.

We observe that green square lies in the box centered with green circle. Hence $[f, i]$ on $X \times \{t_i\}$ and $[h, i]$ on $X \times \{t_{i+1}\}$ are joined in the discrete bifurcation diagram. The birth and death algorithm gives strong connection between $[f, i]$ on $X \times \{t_i\}$ and $[h, i]$ on $X \times \{t_{i+1}\}$.

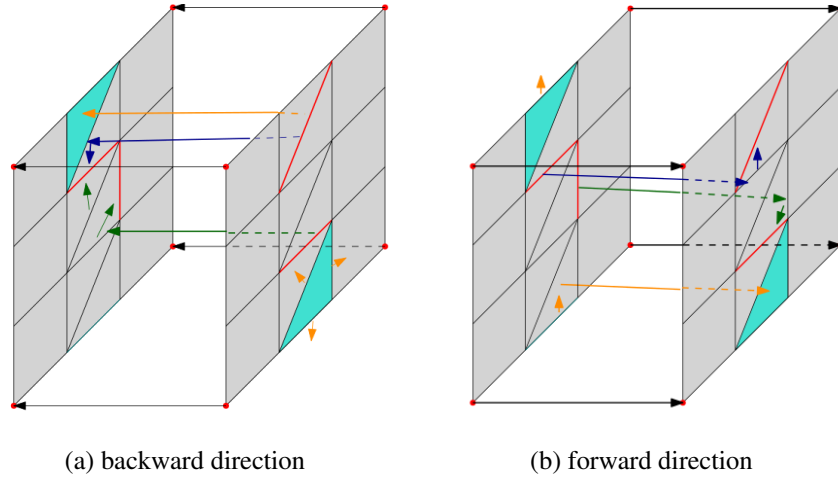


Figure 4.16: Connectivity diagrams associated with the example in figure 4.13

We also check the extended persistence diagrams to say more things about them since they are essential homology classes of dimension 1. Let a_1, a_2 be homological critical values of $[f, i]$ and $[e, f]$ respectively and b_1, b_2 be homological critical values of $[h, i]$ and $[c, e]$ respectively. Note that $a_1 < a_2$ and $b_1 < b_2$. In $X \times \{t_i\}$ the minimum critical cell is paired with the maximum critical cell by the Reeb graph. In the same way, the saddle $[f, i]$ is paired with $[e, f]$. The minimum and the maximum critical cell on $X \times \{t_{i+1}\}$ get paired. Similarly, the saddle $[h, i]$ is paired with $[c, e]$. See figure 4.17.

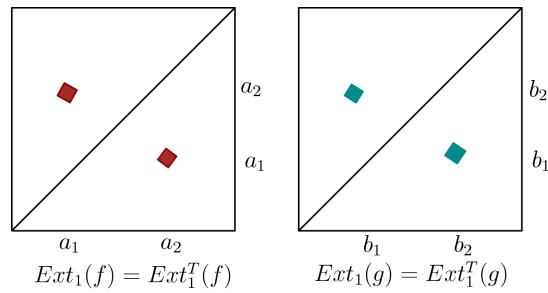


Figure 4.17: Extended persistence diagrams of dimension 1

4.2 Method for the Second Case

Now let us consider the two slices where the cell decompositions are not same as in figure 4.18.

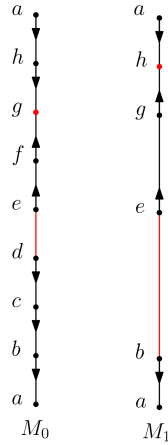


Figure 4.18: A family of discrete gradient fields on circle with different cell decomposition

We make filtrations for M_0 and M_1 . We find the persistence diagrams for each dimension. We compute the bottleneck distance as 0 for 0-dimension and 3 for 1-dimension.

We use the algorithm 2 in [14]. We add a node and draw a vector, then compute bottleneck distance for each dimension. After adding node c on M_1 , the bottleneck distance is 0 for 0-dimension and 2 for 1-dimension. When we add last node f on M_1 , the bottleneck distance is 0 for 1-dimension. We observe that adding node decreases the value of the bottleneck distance for 1-dimension.

Algorithm 2 Algorithm Birth-death 2

```

1: for  $d = 0, \dots, \dim M$  do
2:   for  $i = 0, \dots, r$  do
3:     for all  $\alpha^d$  critical in  $V_i$  do
4:       add a node denoted by  $\alpha$  in layer i
5:       add an edge from the node  $\alpha$  to each node in  $V_{i-1}$  strongly connected
6:     end for
7:   end for
8: end for

```

Let us consider the following two discrete Morse functions on circle. M_1 contains one 0- and one 1-dimensional critical cells and M_2 contains two 0- and two 1-dimensional critical cells.

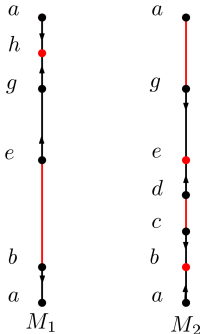


Figure 4.19: Discrete Morse functions on circle with different cell decomposition

Note that the critical cell h on M_1 is a 0-dimensional essential homology class and $[b, e]$ is a 1-dimensional essential homology class. On M_2 , b is a 0- and $[c, d]$ is a 1-dimensional essential homology class. The critical cell e has a persistence pair $[g, a]$.

The refinements of M_1 and M_2 are $M_{3/2}$ as seen in figure 4.20(b). The bottleneck distance of dimension 1 decreases when the nodes c, d are added on 1-dimensional critical cell $[b, e]$ on M_1 , because we divide the 1-dimensional critical cell. The bottleneck distance of 0- dimension is same before and after refinement since there is no division on the 0 dimensional critical cell.

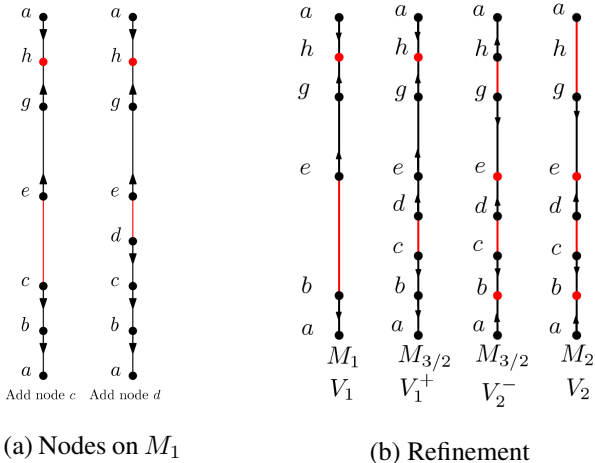


Figure 4.20: Refinement process

In this part, we want to state a proposition as follows:

Proposition 4.2.1. *Let M be a circle and suppose that we have a discrete Morse function $f_{t_i} : M \rightarrow \mathbb{R}$ defined on M . Let the simplicial complex $M_i = M \times \{t_i\}$ and $M_{i+1} = M \times \{t_{i+1}\}$ be the first and second slices respectively. Then 0-dimensional critical cell on slice M_{i+1} must go to the one of the 0-dimensional critical cell on M_i and vice versa.*

Proof. Let take two slices M_i and M_{i+1} . Suppose e_{i+1} is the 0-dimensional critical cell on M_{i+1} and does not go to any critical cells on M_i . This implies that there must be 1-dimensional critical cells on each side of regular cell e_i on M_i . But this forces e_i to be the critical cell as seen in figure. \square

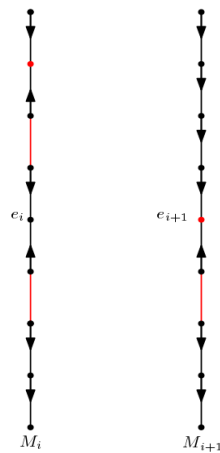


Figure 4.21: Discrete Morse functions on circle with same cell decomposition

4.3 Application

We use leukemic cells in blood of leukemic mouse as data set [2]. Leukemia is monitored by increase in leukemic cells in blood and considered positive when leukemic cell counts exceeded $6 \times 10^3 \text{ cells/mm}^3$. Leukemic mouse is injected doses of medicine ranging from 0 to 100 mg/kg .

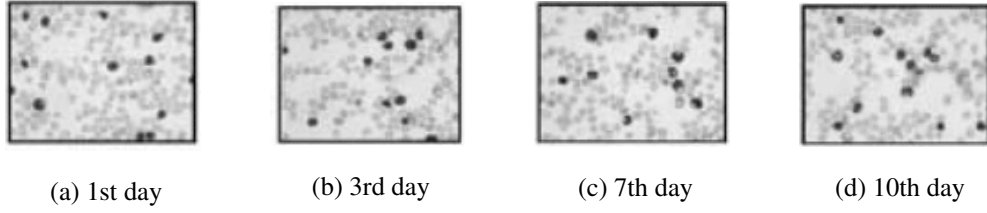


Figure 4.22: Blood of leukemic mouse

In figure 4.22, each image is in png format and is 108 px wide and 80 px height and is taken in 10 days. Each of them is loaded in Matlab. With `imread` and `impixelregion` commands in Matlab, the resolution of the 2D grayscale images is obtained. A function on the image is defined by $f : M \times \{t_j\} \rightarrow \mathbb{Z}$ where M is a rectangular shape with the resolution of the image (the number of pixels) and $j = i - 1, i, i + 1, i + 2$. The value of pixel increases as the colour changes from dark to white.

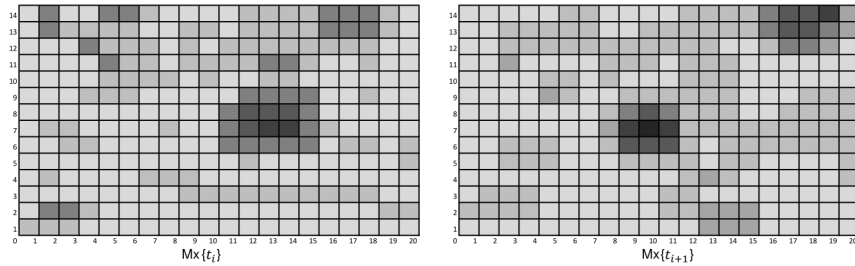


Figure 4.23: Image of leukemic cell

Let $M \times \{t_i\}$ and $M \times \{t_{i+1}\}$ be the slices of leukemic cells monitored in 3-rd and 7-th day respectively. See figure 4.23. We take other adjacent slices $M \times \{t_{i+1}\}$ and $M \times \{t_{i+2}\}$ of the 7-th and 10-th day as in figure 4.24.

In this application the sequence of images are modelled with a vertex for each pixel ranging from 39 to 255 and each adjacent vertex is connected by edge. The extended

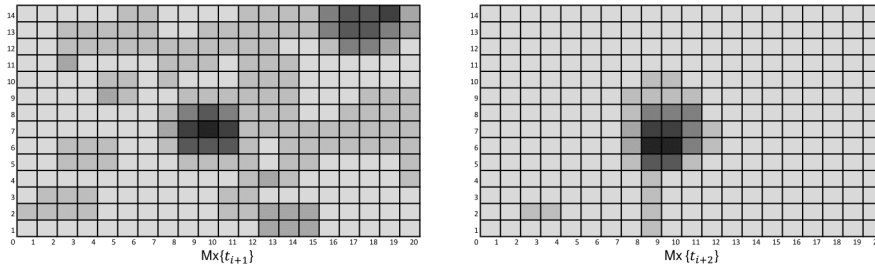


Figure 4.24: Image of leukemic cell

discrete gradient vector fields are found by using the algorithm in [15]. The birth and death algorithm gives the discrete bifurcation diagram of the minimal vertices in a sequence of images. In figure 4.25, the black lines show the strong connections between critical cells and red lines show the connection between them in one way.

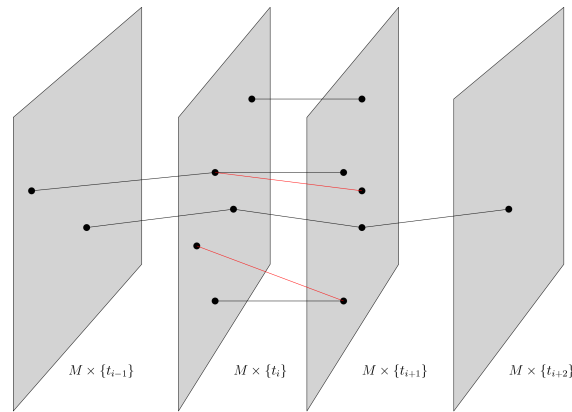


Figure 4.25: Connectivity diagrams associated with the application

For our algorithm, we take adjacent slices. The pixel values of the vertices from 39 to 255 are ordered. The filtration for each slice is obtained by using the sublevel sets which turns out persistence diagrams. Within each interval (t_j, t_{j+1}) $j = i-1, \dots, i+2$, we connect the points in the figures at $t = t_j$ and $t = t_{j+1}$. Tracking the lines gives the discrete bifurcation diagrams.

Since the images are monitored in a short period and nothing is injected to the mouse, there are no big changes among the images. For this reason, the result obtained by the application of the birth and death algorithm and our algorithm is the same when considering the strong connection between critical cells.

In this part we state the outline of the algorithm which draws the discrete bifurcation

diagrams by using persistence diagrams.

Output: Discrete Bifurcation Diagrams

Input: An n -dimensional simplicial complex K .

a) Let $f : K \times \{t_i\} \rightarrow \mathbb{R}$ be discrete Morse function on K and c_i be the function values of the simplices on $K \times \{t_i\}$ with order $-\infty = c_0 \leq c_1 \leq \dots \leq c_l$.

Let $g : K \times \{t_{i+1}\} \rightarrow \mathbb{R}$ be discrete Morse function on K and d_i be the function values of the simplices on $K \times \{t_{i+1}\}$ with order $-\infty = d_0 \leq d_1 \leq \dots \leq d_l$.

b)

Algorithm 3 sublevel set of f

```
1: for  $i = 1, \dots, l$  do
2:   if  $c_i \geq c_{i-1}$  then
3:      $K_i = f^{-1}(-\infty, c_i]$  and  $K_{i-1} \subset K_i$ 
4:   end if
5: end for
```

Algorithm 4 sublevel set of g

```
1: for  $i = 1, \dots, l$  do
2:   if  $d_i \geq d_{i-1}$  then
3:      $K_i = g^{-1}(-\infty, d_i]$  and  $K_{i-1} \subset K_i$ 
4:   end if
5: end for
```

The sublevel set of f consists of all simplices α of $K \times \{t_i\}$ such that $f(\alpha)$ less than or equal to c .

Similarly, the sublevel set of g consists of all simplices β of $K \times \{t_{i+1}\}$ such that $g(\beta)$ less than or equal to d .

c)

Algorithm 5 Persistence Pairing for each slice

```
1: for  $i = 1, \dots, l - 1$  do
2:   if  $K_{i+1} \setminus K_i = \sigma_{i+1}$  is a negative simplex then
3:     pair the youngest positive simplex with  $\sigma_{i+1}$ 
4:   else
5:     a positive simplex with no persistence pair becomes an essential homology class
6:   end if
7: end for
```

The persistence pairs are represented as a point on the persistence diagrams for each dimension $p < n$.

d) Let $X = Dgm_p(f)$ and $Y = Dgm_p(g)$ be the persistence diagrams of f and g respectively. Compute the bottleneck distance $d_B(X, Y) = \inf_{\rho: X \rightarrow Y} \sup_{x \in X} \|\rho(x) - x\|$ where $\rho: X \rightarrow Y$.

e) Check that for each dimension p , the bottleneck distance between the persistence diagrams X and Y is bounded from above by the L_∞ - norm of difference of functions, formally, $d_B(X, Y) \leq \|f - g\|_\infty$. Then state that persistence diagrams are stable.

f) Draw a box of side length twice the bottleneck distance centered at the (m_i, n_i) which corresponds to the critical cell in the persistence diagram, X .

Algorithm 6 Connection of the critical cells

```
1: for  $i = 1, \dots, m$  do
2:   if  $(r_i, s_i)$  in  $Y$  lies in the box centered at the  $(m_i, n_i)$  in  $X$  then
3:     draw line between corresponding critical cells
4:   end if
5: end for
```

g) To find the persistence pair of essential homology class and n -dimensional class, use Duality Theorem to extend persistence homology sequence. Superimpose two persistence diagrams and follow the step (f). If the cell decompositions are not same then we need to make refinements by using the following argument [14]:

Algorithm 7 Algorithm Birth-death 2

```
1: for  $d = 0, \dots, \dim K = n$  do  
2:   for  $j = 0, \dots, r$  do  
3:     for all  $\beta^d$  critical in  $V_j$  do  
4:       add a node denoted by  $\beta$  in layer  $j$   
5:       add an edge from the node  $\beta$  to each node in  $V_{j-1}$  strongly connected  
6:     end for  
7:   end for  
8: end for
```

When the refinements are accomplished, the above 7 steps are followed.

4.4 Conclusion

In this thesis we drew the combinatorial version of the bifurcation diagram in smooth Morse theory by using persistence homology. The method is compared with the birth and death algorithm [14]. We found that when persistence diagrams were stable, the discrete bifurcation diagrams were same as the diagrams obtained from the birth and death algorithm [14]. As we implement our method, we observe some benefits, such as for an n -dimensional simplicial complex if the persistence diagrams are stable, we determine the persistence pair of an m -dimensional critical cell by the Duality Theorem [5]. Hence if we know that an m -cell on one of the slice goes to an m -cell on the next slice, we can say their corresponding dual cells are going to each other. This makes computation more efficient.

Another advantage of our method is that if we need to track 0-dimensional critical cell on the slices where cell decompositions are not same, we see that the process of refinements does not change the bottleneck distance of dimension 0. Therefore we draw discrete bifurcation diagram of dimension 0 without making refinements. We can find the persistence diagrams for the higher dimension without making any refinements and this gives us some clues about drawing discrete bifurcation diagrams. We observe that the bottleneck distance decreases under the process of refinements for dimension greater than 0. When the refinements are accomplished we can apply our method to find discrete bifurcation diagrams.

Besides advantages of our method there is an restriction about the application of it. It requires compact manifold with boundary to implement Lefschetz duality when we need extended persistence homology.

REFERENCES

- [1] P. Bubenik. Statistical topological data analysis using persistence landscapes. pages 77–102., 2015. <https://arxiv.org/pdf/1207.6437.pdf>.
- [2] F. Cano, R. Pannel, G. A. Follows, and T. H. Rabbitts. Preclinical modeling of cytosine arabinoside response in mll-enl translocator mouse leukemias. 2008.
- [3] F. Chazal and B. Michel. An introduction to topological data analysis: fundamental and practical aspects for data scientists. 2017. <https://arxiv.org/pdf/1710.04019>.
- [4] D. Cohen-Steiner, H. Edelsbrunner, and J. Harer. Stability of persistence diagrams. 2005. <http://pub.ist.ac.at/~edels/Papers/2007-J-01-StabilityPersistenceDiagrams.pdf>.
- [5] D. Cohen-Steiner, H. Edelsbrunner, and J. Harer. Extending persistence using poincaré and lefschetz duality. 2009.
- [6] D. Cohen-Steiner, H. Edelsbrunner, and D. Morozov. Vines and vineyards by updating persistence in linear time. page 119–134., 2006. <http://pub.ist.ac.at/~edels/Papers/2006-P-04-VinesVineyards.pdf>.
- [7] H. Edelsbrunner and J. Harer. *Computational Topology. An Introduction*. American mathematical society, Providence, Rhode Island, 2010.
- [8] H. Edelsbrunner and J. Harer. *A short course in Computational Geometry and Topology*. Springer Cham Heidelberg New York Dordrecht London, 2014.
- [9] H. Edelsbrunner, D. Letscher, and A. Zomorodian. Topological persistence and simplification. 28:511–533., 2002. <http://www.math.uchicago.edu/~shmuel/AAT-readings/Data%20Analysis%20/Edelsbrunner-Letscher-Zomordian.pdf>.
- [10] R. Forman. Morse theory for cell complexes. *Adv. Math.*, 134:90–145, 1998.

- [11] R. Forman. A user's guide to discrete morse theory. *Sem. Lothar. Combin.*, 48:35, 2002. <https://www.maths.ed.ac.uk/~v1ranick/papers/forman1.pdf>.
- [12] A. Hatcher. *Algebraic Topology*. Cambridge University Press, Cambridge, 2002. <https://pi.math.cornell.edu/~hatcher/AT/AT.pdf>.
- [13] G. Jerse and N. M. Kosta. Tracking features in image sequences using discrete morse functions. 1(1):27-32, 2010. <https://core.ac.uk/download/pdf/51389344.pdf>.
- [14] H. King, K. Knudson, and N. M. Kosta. Birth and death in discrete morse theory. 2008. <https://arxiv.org/abs/0808.0051>.
- [15] H. King, K. Knudson, and N. Mramor. Generating discrete morse functions from point data. 2005.
- [16] K. P. Knudson. *Morse Theory Smooth and Discrete*. World Scientific Publishing Co.Pte.Ltd. 5 Toh Tuck Link, Singapore 596224, 2015.
- [17] J. Milnor. *Morse Theory*. Princeton Univ. Press, New Jersey, 1963. <https://www.maths.ed.ac.uk/~v1ranick/papers/milnmors.pdf>.
- [18] M. Morse. The foundations of the calculus of variations in the large in m-space. 31(3):379–404, 1929. https://www.jstor.org/stable/1989343?seq=1#page_scan_tab_contents.
- [19] J. R. Munkres. *Elements of Algebraic Topology*. Addison Wesley, Menio Park, California, 1984. <http://webmath2.unito.it/paginepersonali/sergio.console/Dispense/topology%20%20Ed%20-%20James%20Munkres.pdf>.
- [20] V. Robins, P. J. Wood, and A. P. Sheppard. Theory and algorithms for constructing discrete morse complexes from grayscale digital images. 2010.

CURRICULUM VITAE

PERSONAL INFORMATION

Surname, Name: Örnek, Türkmen

Nationality: Turkish (TC)

Date and Place of Birth: 25.04.1969, Sivas

Marital Status: Single

Phone: 0 312 2987000

EDUCATION

Degree	Institution	Year of Graduation
M.S.	Cornell University	1997
B.S.	METU	1992
High School	Deneme High School	1987

PROFESSIONAL EXPERIENCE

Year	Place	Enrollment
2018	Higher Educational Council	Programmer
2001	Netsoft	Microsoft System Engineer
2000	Abant Izzet Baysal University	Research and Teaching Assistant
1994	Abant Izzet Baysal University	Research and Teaching Assistant